

Modelling of Photovoltaic Water Pumping System using Frequency Control of Inverter

A THESIS SUBMITTED IN PARTIAL FULFILLMENT OF THE
REQUIREMENTS FOR THE DEGREE OF

Bachelor of Technology in
Electrical Engineering

By

Rosan Maria (108EE021)

Debayan Chakraborty (108EE080)

Sudeep Kumar Khuntia (108EE082)

Under the supervision of

Prof. S. Samanta



Department of Electrical Engineering
National Institute of Technology, Rourkela

May, 2012



National Institute of Technology, Rourkela

CERTIFICATE

This is to certify that the thesis entitled ‘**Modelling of Photovoltaic Water Pumping System using Frequency Control of Inverter**’ submitted by **Rosan Maria (108EE021), Debayan Chakraborty (108EE080) and Sudeep Kumar Khuntia (108EE082)** in the partial fulfillment of the requirement for the degree of **Bachelor of Technology in Electrical Engineering**, National Institute of Technology, Rourkela, is an authentic work carried out by them under my supervision.

To the best of my knowledge the matter embodied in the thesis has not been submitted to any other university/institute for the award of any degree or diploma.

Date:
Rourkela

Prof. S. Samanta
Dept. of Electrical Engineering
National Institute of Technology
Rourkela-769008, Orissa

ACKNOWLEDGEMENT

We would like to thank NIT Rourkela for giving us the opportunity to use their resources and work in such a challenging environment. .

First and foremost we take this opportunity to express our deepest sense of gratitude to our guide Prof. S. Samanta for his able guidance during our project work. This project would not have been possible without his help and the valuable time that he has given us amidst his busy schedule.

We would also like to extend our gratitude to our friends and senior students of this department who have always encouraged and supported us in doing our work. We would like to thank all the staff members of Department of Electrical Engineering who have been very cooperative with us.

Last, but not least, we would like to thank the authors of various research articles and book that we referred to during the course of the project.

Rosan Maria (108EE021)

Debayan Chakraborty (108EE080)

Sudeep Kumar Khuntia (108EE082)

ABSTRACT

The depletion of fossil fuels and the increasing demand of energy have led to discovering new and supplement sources. In this direction the non conventional sources of energy have proved to be a great supplement. Not only that, few of these sources are the only solution to the power requirement where conventional power generation is not possible or its transmission from the source to that point is too costly. In such cases the power generation based on any of the non conventional source must be efficient to its maximum. In this project an application specific photovoltaic power generation system is designed along with a control mechanism which assists in extraction of increased power at any level of insolation than the normal mode of operation which includes constant frequency inverter operation. The primary use of PV system is usually in the process of water pumping for irrigation and other domestic application. Thus the system designed here is a “FREQUENCY CONTROL BASED WATER PUMPING SYSTEM”. The chief components of this system includes a PV array, a 3 Phase 180 degree mode voltage source inverter, a 3 phase induction motor and a centrifugal pump. Besides this there is a microprocessor based control block which sends the inverter the required control signal to help it track the maximum power. The complete project is based on the Simulink models and their simulation results which are expected to represent the real world components to the closest proximity.

CONTENTS

CERTIFICATE.....	ii
ACKNOWLEDGEMENT.....	iii
ABSTRACT.....	iv
TABLE OF CONTENTS.....	v
LIST OF FIGURES.....	vi
CHAPTER 1: Introduction.....	1
CHAPTER 2: Modelling of various subsystems.....	3
2.1.The Photovoltaic cell.....	3
2.2.The 180 degree mode Voltage Source Inverter.....	6
2.3.The Second order filter.....	10
2.4. The Induction motor.....	11
2.5. The Centrifugal pump.....	14
CHAPTER 3: Control algorithm.....	15
CHAPTER 4: Stepwise realization of the MPPT Model.....	17
4.1.Sizing of various components.....	17
4.2.Design of Inverter.....	19
4.3.Modelling of the PV array.....	21
4.4.Connection of Motor.....	24
4.5.Design of Filter.....	27
4.6.Connection of Centrifugal pump.....	31
4.7.Implementation of the Control block.....	36
CHAPTER 5: Conclusion.....	41
REFERENCES.....	42

LIST OF FIGURES

S.no.	Description	Page no.
1	<i>The basic model of the PV array fed water pumping system</i>	(Introduction)
2.1.1	<i>Single Diode model of solar cell</i>	3
2.1.2	<i>Current versus voltage graph of PV array</i>	5
2.1.3	<i>Power versus voltage graph of PV array showing the maximum power point locus</i>	5
2.1.4	<i>Power versus current graph of PV array</i>	6
2.2.1	<i>Figure showing a six-step IGBT connected to a DC source and a 3phase load</i>	7
2.2.2	<i>Figure showing simulation result of Fig. 2.2.1 (Line voltage versus time)</i>	9
2.2.3	<i>Figure showing simulation results of Fig. 2.2.1 (Phase voltage versus time)</i>	10
2.4.1	<i>Per phase equivalent circuit of Induction motor</i>	11
2.4.2	<i>Figure showing the DC representation of the system</i>	13
4.2.1	<i>Figure showing a six-step IGBT connected to a DC source and a 3phase load</i>	19
4.2.2	<i>Figure showing simulation result of Fig. 4.2.1 (Line voltage versus time)</i>	20
4.2.3	<i>Figure showing simulation result of Fig. 4.2.1 (Phase voltage versus time)</i>	20
4.3.1	<i>Simulink model of the PV array</i>	21
4.3.2	<i>Figure showing voltage and current of the PV array model of Fig. 4.3.1</i>	22
4.3.3	<i>Simulink model of the PV array connected to the inverter</i>	22
4.3.4	<i>Simulation result of Fig. 4.3.3 (Line voltage versus time)</i>	23
4.3.5	<i>Simulation result of Fig. 4.3.3 (Phase voltage versus time)</i>	23
4.4.1	<i>Simulink model showing the 3Phase induction motor</i>	24

	<i>connected to the model of Fig.4.3.3</i>	
4.4.2	<i>Simulation results of Fig. 4.4.1 showing the Line volatage versus time</i>	24
4.4.3	<i>Simulatiuon results of Fig.4.4.1 showing the torque and speed versus time</i>	25
4.4.4	<i>Simulatiuon results of Fig.4.4.1 showing the stator current versus time</i>	25
4.4.5	<i>Simulatiuon results of Fig.4.4.1 showing the stator volatge versus time</i>	26
4.4.6	<i>Simulatiuon results of Fig.4.4.1 showing the FFT analysis of the Line voltage</i>	26
4.5.1	<i>Simulink model showing the second-order filter connected to the model of Fig. 4.4.1</i>	27
4.5.2	<i>Simulatiuon results of Fig.4.5.1 showing the Line volatage versus time</i>	28
4.5.3	<i>Simulatiuon results of Fig.4.5.1 showing the stator voltage versus time</i>	28
4.5.4	<i>Simulatiuon results of Fig.4.5.1 showing the stator current versus time</i>	29
4.5.5	<i>Simulatiuon results of Fig.4.5.1 showing the Torque versus time and Speed versus time</i>	29
4.5.6	<i>Simulatiuon results of Fig.4.5.1 showing the FFT analysis of Line volatage</i>	30
4.5.7	<i>Detailed structure of the filter subsystem used in model of Fig.4.5.1</i>	30
4.6.1	<i>Connection of Centrifugal pump to the model of Fig.4.5.1</i>	31
4.6.2	<i>Detailed structure of the Centrifugal pump subsystem of Fig.4.6.1</i>	32
4.6.3	<i>Simulatiuon results of Fig.4.6.1 showing the Power of the motor,electromagnetic torque and volumetric flow rate</i>	32

4.6.4	<i>Simulatiuon results of Fig.4.6.1 showing the Line volatage versus time</i>	33
4.6.5	<i>Simulatiuon results of Fig.4.6.1 showing the electromagnetic torque and rotor speed versus time</i>	33
4.6.6	<i>Simulatiuon results of Fig.4.6.1 showing the stator current versus time</i>	34
4.6.7	<i>Simulatiuon results of Fig.4.6.1 showing the stator volatage versus time</i>	34
4.6.8	<i>Simulatiuon results of Fig.4.6.1 showing the rotor speed,torque and the pump flow rate</i>	35
4.6.9	<i>Simulatiuon results of Fig.4.6.1 showing the FFT analysis of the line voltage</i>	35
4.7.1	<i>Connection of the Control block to the model of Fig. 4.6.1</i>	36
4.7.2	<i>Detailed structure of the control block of Fig.4.7.1</i>	37
4.7.3	<i>Simulatiuon results of Fig.4.7.1 showing the Line volatages versus time</i>	37
4.7.4	<i>Simulatiuon results of Fig.4.7.1 showing the stator current versus time</i>	38
4.7.5	<i>Simulatiuon results of Fig.4.7.1 showing the stator current versus time and stator voltage versus time</i>	38
4.7.6	<i>Simulatiuon results of Fig.4.7.1 showing the rotor speed versus time</i>	39
4.7.7	<i>Simulatiuon results of Fig.4.7.1 showing the Volumetric flow rate, rotor speed and the power of the motor</i>	39
4.7.8	<i>Simulatiuon results of Fig.4.7.1 showing the time period being fed by the control block into the inverter and the irradiation versus time</i>	40

CHAPTER 1

INTRODUCTION

I. INTRODUCTION:

The model designed consists of a PV array, a 3 Phase 180 degree mode voltage source inverter, a 3 phase induction motor and a centrifugal pump. The power increment is done by frequency control of inverter which is done with the help of a microprocessor based control block.

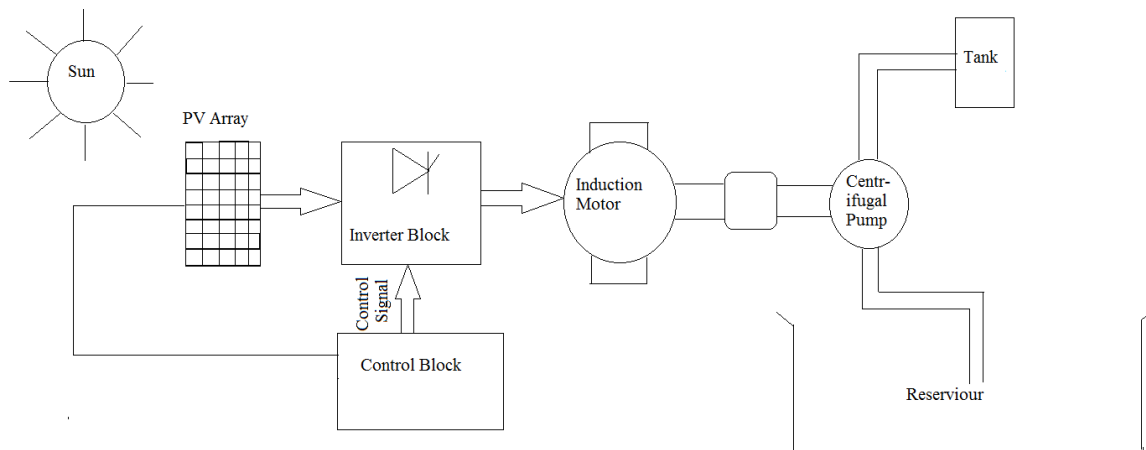


Fig. 1

Since it is an application specific model the sizing of the various components is completely based on a particular specification. First the average insolation period in a day is estimated and the water requirement in a day is predicted. Based on that the water pumping speed is calculated and the required power rating of the centrifugal pump is achieved. This gives us an idea regarding the rating of the 3 phase induction motor to be used. The individual rating of the

available thyristors helps us decide the total number of thyristor to be used in the inverter module. A margin of 30-50% in the positive scale is taken for the power rating of the PV array. The control mechanism is based on simple frequency control for power variation in case of 3 phase induction motor. Based on the value of the insolation we get a particular value of frequency on which the system when operated gives power more than that in case of constant frequency operation. Unlike the conventional algorithms used earlier for achieving maximum power for the PV array this method is completely different in a way in which the inverter helps in increasing the power along with the induction motor and the centrifugal pump.

CHAPTER 2

MODELLING OF VARIOUS SUBSYSTEMS

2.1. THE PV ARRAY

The typical representation of a solar cell is based on a single diode model shown below.

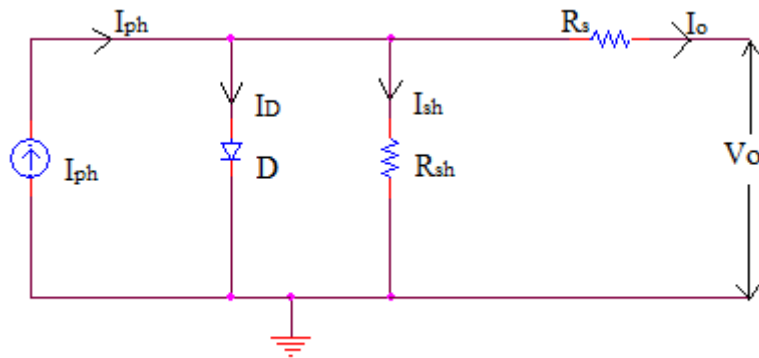


Fig. 2.1.1

I_{ph} represents the photo current.

The diode represents the positive bias of the PN junction diode and I_d the diode current.

I_{sh} represents the leakage current due to electron hole recombination.

I_o is the load current fed into the load.

$$I_{ph} = I_d + I_{sh} + I_o$$

$$I_d = I_o [e^{\frac{qV_o}{n k T}} - 1]$$

q = charge of electron

V_o = forward biased voltage (0.7V for Si and 0.3V for Ge)

N = Ideality factor = 1.92

k = Boltzmann constant = $1.38 \times 10^{-23} \text{ kg m}^2 \text{ s}^{-2} \text{ K}^{-1}$

T = temperature in Kelvin

Solar cell is basically a normal PN junction diode directly converting thermal radiation of sun in to electrical energy. It has large surface and junction area. Immobile ions form the barrier at the PN junction. The voltage of this barrier is around 0.7V for Silicon and 0.3V for Germanium. As the electron hole pairs increase in number the PN junction decreases. After recombination, current flows from N to P layer. A single solar cell generates a maximum of 0.65V.

The output voltage and the output current depends on temperature and solar radiation. The efficiency of the solar cell depends on the material technology used for making solar cell. The monocrystalline silicon used earlier for power generation had efficiency in the range of 15 to 20%. But with use of thin film technology for solar cell fabrication the efficiency has increased. 75 sq.cm of surface area of PN junction generates 1.5W power.

The solar cell model provided in the MATLAB acts as an infinite power source and hence its power cannot be regulated to the practical maximum. Therefore a MATLAB EMBEDDED FUNCTION has been used in its place to achieve operation at an increased power point.

The following graphs show the various characteristics of the PV array. The temperature dependence has not been considered to reduce the complexity.

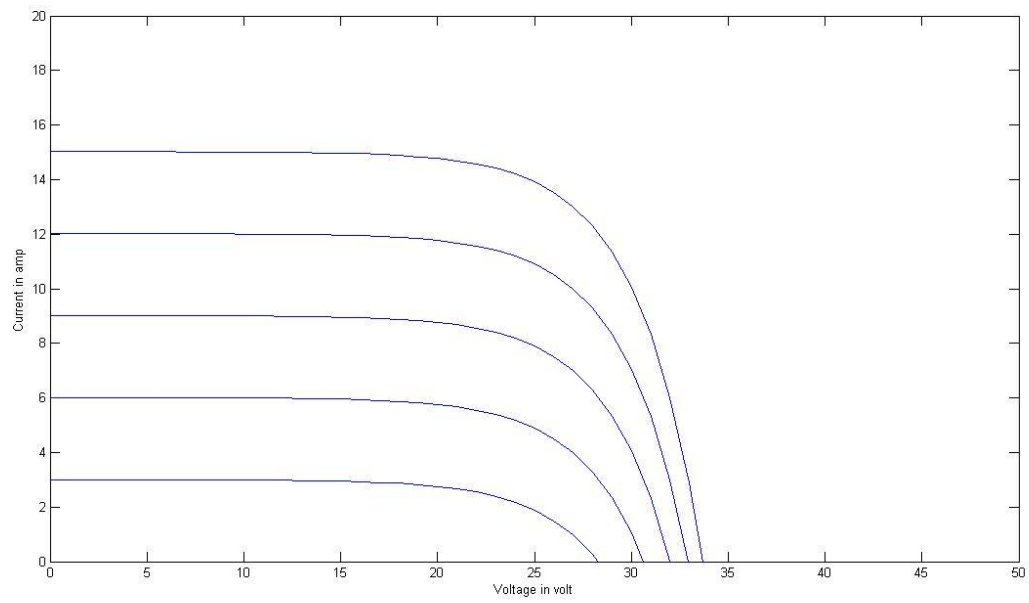


Fig. 2.1.2

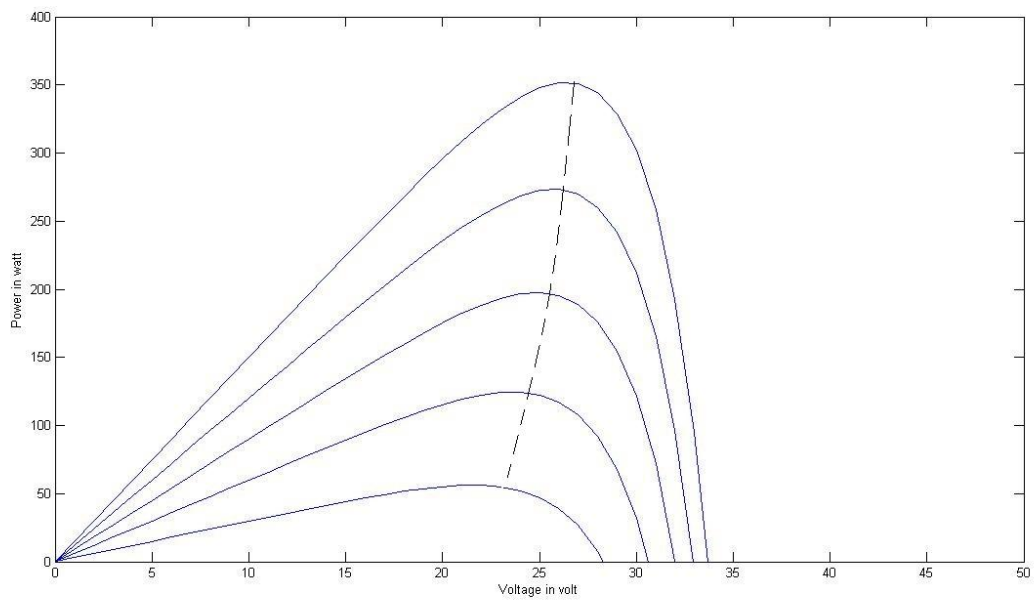


Fig. 2.1.3

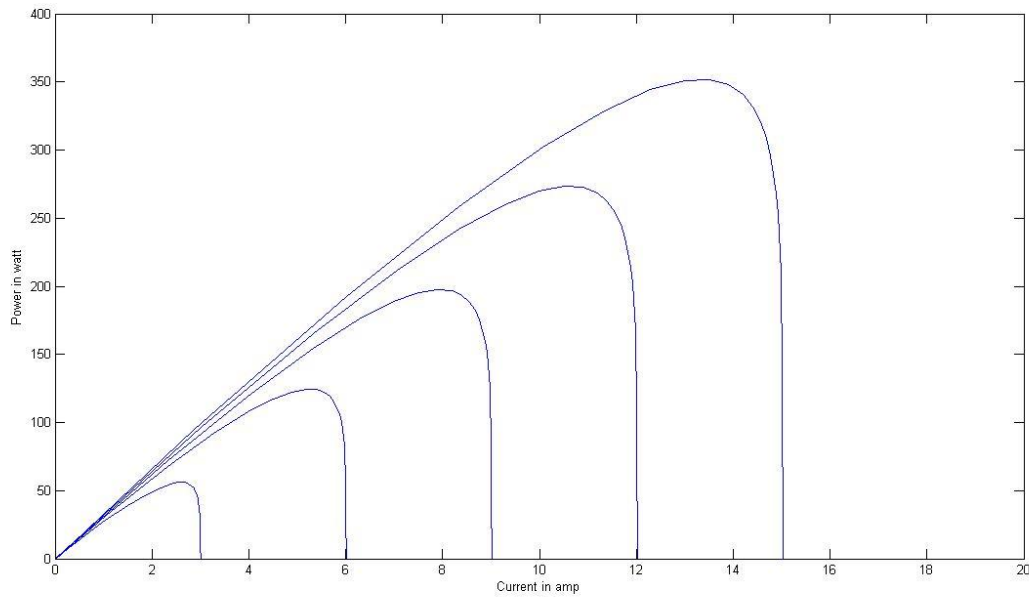


Fig. 2.1.4

The open circuit voltage has a logarithmic relation with the solar irradiation while the short circuit current varies linearly with it. Thus, as solar irradiation increases the short circuit current also increases but the open circuit voltage cannot go beyond 0.65 volt. The maximum power is obtained at knee point of the curve 1. As the solar irradiation increases, P_{max} increases due to increase in short circuit current. The aim of any control block aimed at increasing power is by variation of voltage or current.

2.2 THE 180 DEGREE MODE VOLTAGE SOURCE INVERTER

The DC voltage obtained from the PV array is converted to AC voltage with the help of inverter. A voltage source inverter provides a firm link voltage across the motor terminals. While the load current adjust itself according to the impedance of the motor. Here a six-step 180 degree mode Voltage Source inverter is used. The prime reason behind using a six-step inverter is only to minimize the switching losses since the phase voltage in this case is a six-step wave. The use of IGBTs is preferred because of increased development in the power rating of the IGBTs. Besides

this the use of thyristors needs additional commutation circuitry which makes the circuit further complex in control.

According to the convention a step is a change in the firing sequence of the IGBTs. For a six step inverter each step corresponds to 60 degree interval in a single cycle of 360 degree which means the IGBTs required to be gated at a regular interval of 60 degree in the correct sequence to obtain a 3 phase AC voltage at the output terminals. A large capacitor makes the DC voltage constant at the input terminal.

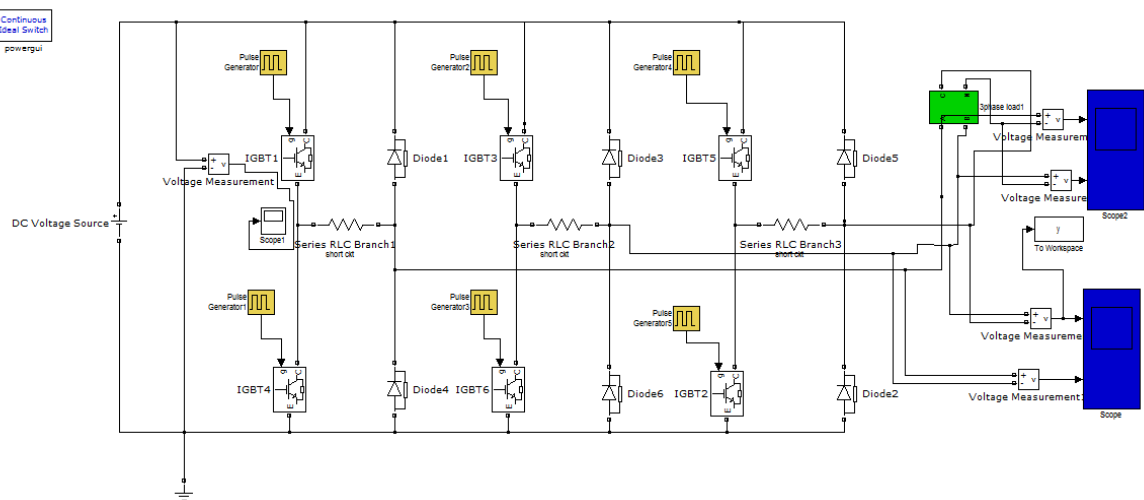


Fig. 2.2.1

In the 180 degree mode VSI each IGBT conducts for 180 degree of a cycle. The IGBTs are paired in each arm (IGBT1, IGBT4; IGBT3, IGBT6; IGBT5, IGBT2). Each IGBT in each arm conducts for 180 degree and the next for another 180 degree of the cycle. IGBTs in the upper group (IGBT1, IGBT3 and IGBT5) conduct for an interval of 120 degree and same is the case for lower group IGBTs.

At $\omega t = 0$, IGBT1 is gated which conducts for 180 degree and then at $\omega t = 180$ degree IGBT4 is gated. The upper arm IGBT3 is gated at $\omega t = 120$ degree and its corresponding IGBT6 after 180 degree of its gating. Same applies for IGBT5 which is gated at $\omega t = 240$ degree and IGBT2 180 degree after it. Thus in step 1, IGBT5, IGBT6, and IGBT1 are conducting. Load terminal A and C are connected to the positive bus of the DC source and B to the negative.

During step1, $0 \leq \omega t < 60$, IGBT5, IGBT6 and IGBT1 are conducting,

$$\text{Thus, current } i = \frac{Vs}{Z + \frac{Z}{2}} = \frac{2Vs}{3Z}$$

And the line to neutral voltages are

$$V_{an} = V_{cn} = i * Z / 2 = Vs / 3$$

$$\text{and } V_{bn} = i * Z = 2Vs / 3$$

STEP	IGBTs Conducting	IGBTs connected to positive DC bus	IGBTs connected to negative DC bus	I_{an}	I_{bn}	I_{cn}
1	5, 6, 1	1, 5	6	$(Vs/3)$	$(-2Vs/3)$	$(Vs/3)$
2	6, 1, 2	1	2, 6	$(2Vs/3)$	$(-Vs/3)$	$(-Vs/3)$
3	1, 2, 3	1, 3	2	$(Vs/3)$	$(Vs/3)$	$(-2Vs/3)$
4	2, 3, 4	3	2, 4	$(-Vs/3)$	$(2Vs/3)$	$(-Vs/3)$
5	3, 4, 5	3, 5	4	$(-2Vs/3)$	$(Vs/3)$	$(Vs/3)$
6	4, 5, 6	5	4, 6	$(-Vs/3)$	$(-Vs/3)$	$(2Vs/3)$

The phase voltages have six steps per cycle while line voltages are one positive and one negative pulse (each of 120 degree duration) per cycle. The diodes are connected to allow the flow of current through them during a reactive load.

The three line output voltages expressed in Fourier Series are :

$$V_{ab} = \sum_{n=1,3,5}^{\infty} \frac{4Vs}{n\pi} * \cos \frac{n\pi}{6} * \sin n (\omega t + \pi/6)$$

$$V_{bc} = \sum_{n=1,3,5}^{\infty} \frac{4Vs}{n\pi} * \cos \frac{n\pi}{6} * \sin n (\omega t - \pi/2)$$

$$V_{ca} = \sum_{n=1,3,5}^{\infty} \frac{4Vs}{n\pi} * \cos \frac{n\pi}{6} * \sin n (\omega t + 5\pi/6)$$

For $n = 3$, $\cos(3\pi/6) = 0$. This indicates that the triplen harmonics are absent from the line voltages. These voltages are independent of the nature of load which can be any combination of resistance, inductance and capacitance.

The phase voltage is given by the equation :

$$v_{an} = \sum_{n=6k+1}^{\infty} \frac{2V_s}{n\pi} * \sin n\omega t$$

where $k = 0, 1, 2, \dots$

The following graphs show the output of the inverter.

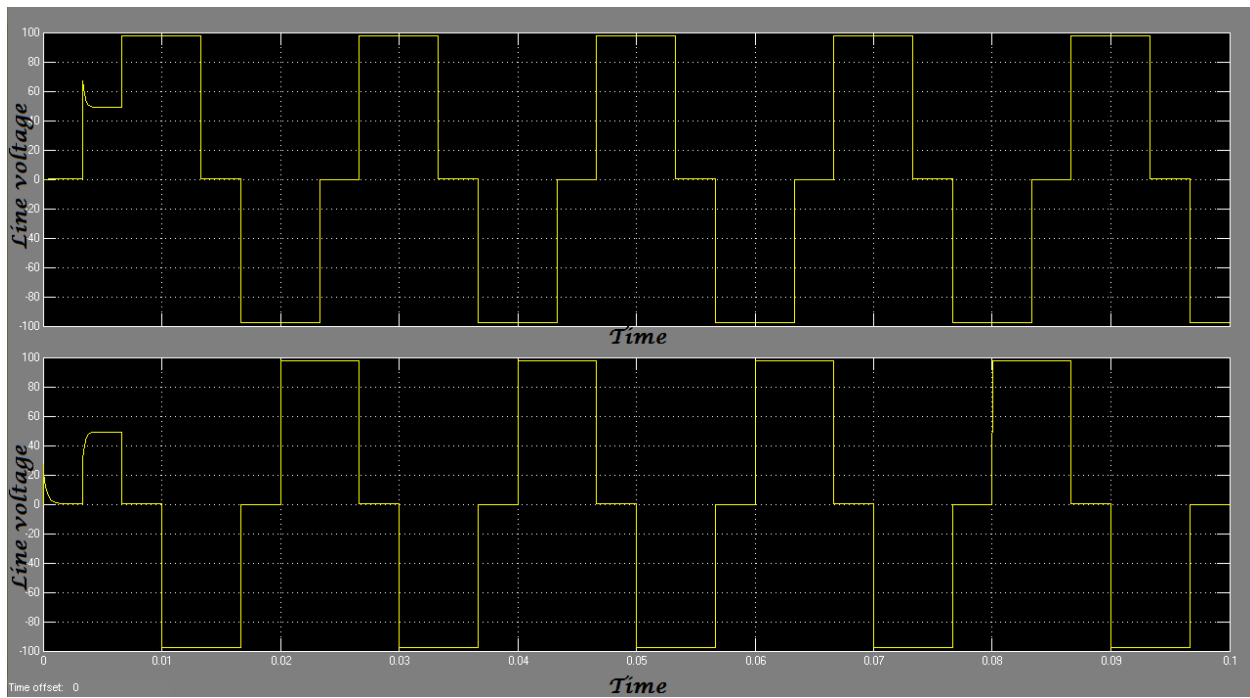


Fig. 2.2.2

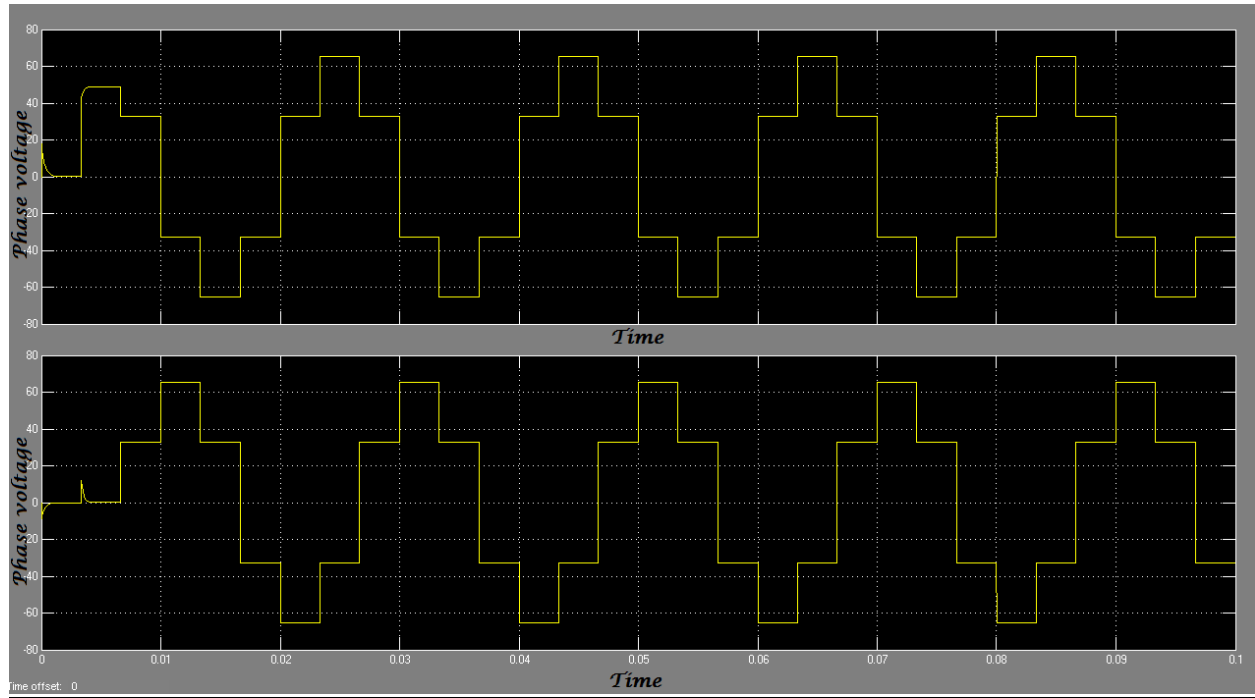


Fig. 2.2.3

2.3. THE SECOND ORDER FILTER

Due to the six-step wave output being fed into the induction motor the response of the motor deteriorates chiefly because of the presence of the harmonics. The lower order harmonics lead to torque pulsations and low speed noises.

Thus, the response of the overall system if required to be improved can be done by introducing filter. And since our aim is only to achieve an approximate sinusoidal wave, we need not require a tuned filter. Instead a low-pass filter with its cut-off frequency slightly higher than the maximum frequency of the inverter block can be used.

The FFT analysis of a signal shows its spectrum which shows the magnitude of various harmonic contents as a percentage of the magnitude of fundamental versus frequency.

The total harmonic distortion is given by THD =

$$\frac{\sqrt{H_2^2 + H_3^2 + \dots + H_N^2}}{\sqrt{H_1^2 + H_2^2 + \dots + H_N^2}} * 100\%$$

2.4. THE INDUCTION MOTOR

The pumping operation is achieved by the centrifugal pump which needs to be coupled with a rotor. Hence an induction motor is used which helps in transferring the power from the inverter to the centrifugal pump via the conversion of electrical energy into mechanical. Here a squirrel-cage induction motor is used whose rotor bars are short-circuited.

When a 3-phase supply is connected to the motor stator winding a rotating magnetic field is produced which rotates at synchronous speed given by

$$N_s = \frac{120f_1}{P}$$

Where f_1 = supply frequency in hertz

P = number of stator poles

The rotor rotates at a speed lesser than the synchronous speed. This gives rise to the concept of slip.

$$\text{Slip } s = \frac{N_s - N_r}{N_s}$$

Where N_r is the rotor speed

Below is the per phase equivalent circuit of an induction motor which helps in determining the various parameters

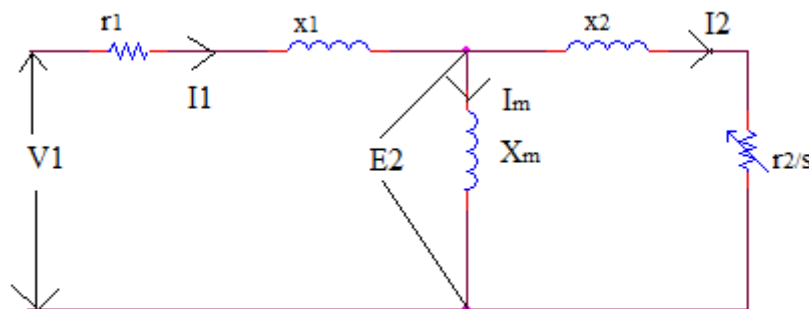


Fig. 2.4.1

In this figure, r_2 = rotor resistance referred to stator, x_2 = rotor leakage reactance referred to stator, $(r_1 + jx_1)$ is the stator leakage impedance and X_m = magnetizing reactance.

For determining shaft torque or shaft power core loss has to be taken into consideration.

The rotor current is given by:

$$I_2 = \frac{V_1}{\left(r_1 + \frac{r_2}{s}\right) + j(x_1 + x_2)}$$

Air gap power is given by:

$$P_g = 3I_2^2 * r_2 / s$$

$$\text{Rotor ohmic loss} = 3I_2^2 * r_2$$

$$\text{Rotor torque} = T_e = P_g / \omega_s = \frac{3}{\omega_s} \left[\frac{V_1^2}{\left(r_1 + \frac{r_2}{s}\right)^2 + (x_1 + x_2)^2} \right] \frac{r_2}{s}$$

The operation of the motor is dependent on the characteristics of the source from which the power is fed, which in this case is a PV array.

As discussed earlier, the PV source when operated near its maximum power point has its characteristics in between the constant voltage and constant current mode of operation. The maximum torque and the slip at which it occurs also varies for the constant voltage and the constant current source.

For the voltage source, the slip is:

$$S = \frac{r_2}{\sqrt{r_1^2 + (x_1 + x_2)^2}}$$

While for the current source, it is:

$$S = \frac{r_2}{(x_1 + x_2)}$$

If the system is represented by an equivalent DC representation as shown in the figure below,

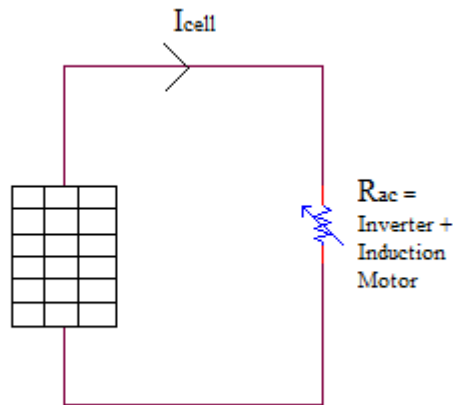


Fig. 2.4.2

the voltage and the current of the motor-inverter relationship has their fundamental components being reflected to the DC side as a variable resistor. The resistance of the variable resistor changes according to the change in slip of the motor which in turn is adjusted by varying the frequency of the inverter. Therefore at any speed, the slip can be made to vary from zero to unity in both the positive and the negative directions by changing the frequency of the inverter.

If the stator resistance is assumed to be negligible then the torque at any frequency depends on the slip frequency $s\omega_g$ and the flux V_s / ω_g applied to the induction motor. According to the per phase equivalent representation it can be concluded that in the low slip region the system impedance will be high thus for the same current the terminal voltage will be higher in the low slip region than that in the high slip region. Hence the source block act as a voltage source in this region. But with the increase in the slip the terminal voltage of the induction motor lowers which tends to make it behave as if in current source mode. At the maximum power point torque speed characteristics of the induction motor thus is between the constant voltage and constant current source mode.

2.5. CENTRIFUGAL PUMP

A centrifugal pump is a rotodynamic pump that creates flow by adding energy to the fluid with the help of a rotating impeller. These are generally used to move liquids through pipes. The entry of the fluid is usually into the pump impeller along or near the rotating axis. It is then accelerated by the impeller making it flow radially outward into the casing. From the casing, fluid enters the downstream pipe and finally discharges to smaller heads. The centrifugal pump converts the mechanical energy of the moving rotor of the induction motor into the kinetic energy of the fluid and also into potential energy by lifting the liquid against gravity to higher altitude.

The input power required to drive a centrifugal pump is dependent on the flow required, the altitude, the length of the pipe and friction characteristics of the pipeline. If P_{in} is the input power required, then

$$P_{in} = \frac{\rho g H Q}{\eta}$$

where:

ρ is the fluid density in kg/m^3

g is the acceleration due to gravity (9.81 m/s^2)

H is the energy added to the flow (m)

Q is the flow rate (m^3/s)

η is the efficiency of the pump

The power is expressed in watt, kilowatt or horsepower. The energy head added to the flow (H) is the sum of the static lift, the frictional head loss and losses due to pipelines of valves. The efficiency may be a combined efficiency of the pump and the motor expressed as a fraction.

CHAPTER 3

CONTROL ALGORITHM

Unlike the typical algorithms used for achieving maximum power, this method employs an indirect tracking algorithm. According to the V-I curve of the PV array, as the voltage increases the current remain constant until the knee point of the curve and after that, with further increase in the voltage the current decreases at a faster rate. According to the power versus voltage graph, the power increases with increase in the voltage until a fixed value of voltage called the optimum voltage after which power decreases with increase in the voltage. For various levels of insolation the maximum power and their corresponding optimum voltage is different which is shown by the dashed line in the P versus V graph. This dashed line is the line of optimization. To achieve this, the terminal voltage of the P-V array needs to be regulated.

The centrifugal pump used here is a typical water pump whose torque varies as the square of its rotor speed and power as a function of the cube of the rotor speed.

$P = k\omega^3$ where 'k' is the pump constant

While the torque equation is

$$T = k\omega^2$$

The torque-speed characteristics of an induction motor for various supply frequency is different and the operating point for the various frequencies are the points that intersect with the torque line of the centrifugal pump. This implies that the power of the pump can be varied by varying the frequency of the motor driving the pump. The supply frequency to the motor is dependent on the switching frequency of the six step inverter. Moreover the operation of the motor and the inverter is dependent on the characteristics of P-V array. Thus the inverter supplies variable frequency AC. This tracking method minimizes the switching losses. Thus at every step the

power of the PV array, the terminal voltage and the DC current need to be fed to the control block which derives the frequency at which the inverter needs to be operated.

As stated earlier the impedance of the motor is dependent on the slip frequency. When the frequency is varied the impedance of the motor varies thus changing the terminal voltage. This voltage change actually helps in tracking the maximum power point.

The steps to be followed for frequency control are:

- The solar irradiation is sensed with the help of a sensor.
- The short circuit current of the PV array holds linear relation with the solar irradiation. Thus if the short circuit current for the rated insolation is known then the short circuit current at any given insolation can be calculated.

$$I_{sc} = I_{scrated} * (I_r / I_{rrated}).$$

$$\text{Where } I_{rrated} = 1000 \text{ watt/m}^2$$

$$I_{scrated} = 3.75 \text{ A}$$

- After calculating the short circuit current the approximate frequency at which maximum power will occur is calculated with the help of the relation

$$f = f_{rated} \left[\frac{I_{sc-cell}}{I_{sc-rated}} \right]^{1/3}$$

- After this the time period is calculated from the simple equation

$$T = 1/f$$

- To achieve maximum power:

This time period can be compared with the previous one. If this time period is greater than the previous one, then the earlier time period is incremented in steps till the desired time period is achieved. Simultaneously the power of the P-V array is checked.

If the slope of the Power v/s Time plot is positive, it indicates that one is heading in the right direction. At a particular point the slope of the above plot changes from positive to zero to negative. The instant this happens the time period needs to be decremented to the point where the slope was zero. This is the corresponding maximum possible power at the given level of insolation.

- The same method is applied if the time period is less than the previous one. But in this case the time period is decremented step wise simultaneously checking for the zero slope of the P-V power plot.

CHAPTER 4

STEPWISE REALIZATION OF THE PUMPING SYSTEM IN SIMULINK ENVIRONMENT

4.1. SIZING OF VARIOUS COMPONENTS

To explain the method of sizing of each component an example has been considered:

*Calculate the power rating of each of the component used in the PV water pumping system required to drive a centrifugal pump that would fill the tank of volume 324000 L in an average solar day of irradiation period 6 hours. The pump is required to deliver water to a height of 20 m through a 15cm diameter pipe and 100 m long. The overall efficiency of the pump is 70% and coefficient of friction $f=0.15$ in the formula $h_f = 4f L V_s^2/d*2g$.*

Solution

Volume = 324000 L

Diameter = 2m

Height = 3.65m

Manhole Size = 510mm

We estimate the average irradiation time to be around 6 hours.

This gives the discharge = (Volume/Average Irradiation Time) = $0.015 \text{ m}^3/\text{s}$

Height = 20m

Diameter of the pipe = 15cm

Length = 100m

Overall Efficiency = 0.7

Coefficient of friction (f) = 0.15

Therefore velocity of water in pipe (V_s) = Discharge/Area of Pipe = 0.8488 m/s

The frictional head loss in Pipe = $(4fL V_s^2/d*2g) = 1.469\text{m}$

The manometric head $H_m = 21.51\text{m}$

Overall Efficiency (η) = $(\rho g Q H_m/1000*S.P.) = 0.7$

S.P. = 4.5KW

This is the power required to drive the centrifugal pump.

So the power of the motor should be around 1.5 times of the above power which gives us the rating of the motor. A typical three-phase induction motor has its line voltage 400V. This would give the current rating of the motor.

After achieving the current, voltage and power rating of the motor, the number of solar cells required in the module can be determined.

r.m.s. value of line voltage : $V_L = \sqrt[3]{(2/3)} V_s = 0.8165 V_s$

where

V_s is the DC link voltage

Each solar cell gives a voltage of 0.65V. Thus number of solar cells required to be connected in series is = $(V_s/0.65)$

Similarly the current rating of the motor divided by the short-circuit current of each cell (3.75A) gives the number of such modules to be connected in parallel.

The phase current in each stator phase of the motor also decides the number of IGBT modules required to be connected in parallel while the voltage rating decides the number of IGBTs required to be connected in series in each module.

With the increased rating of IGBT only one IGBT in a single module can serve the job.

4.2. DESIGN OF INVERTER

The first step is the design of inverter which would convert the DC voltage of the PV array into AC voltage to be fed into the induction motor. A 180 degree mode VSI is used which would act as a source of constant voltage as long as the insolation remains constant. There is no compulsion regarding the use of thyristors as we are not supposed to control the voltage through firing angle control. Rather the use of thyristors would make the circuit more complex due to additional commutation circuitry because the presence of DC source is unabling self commutation. Hence the use of IGBT is preferred. Thus a set of 6 IGBTs have been used numbered from 1 to 6 according to the sequence of gating. Since at present it is being designed for a constant insolation, the time period has been set to 0.02 seconds owing to a frequency of 50 hertz. The pulse width has been set to 50% since the IGBTs remain on as long as the pulse is present and because it is 180 degree so each IGBT got to remain on for half of the time period.

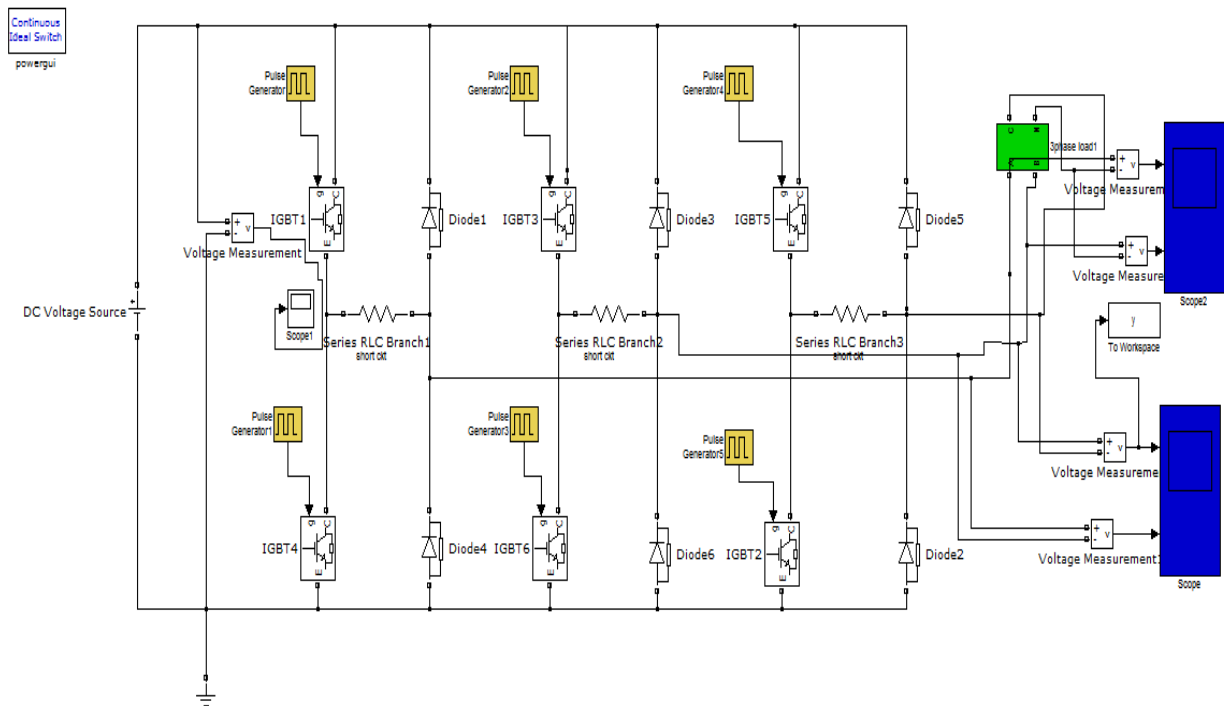


Fig. 4.2.1

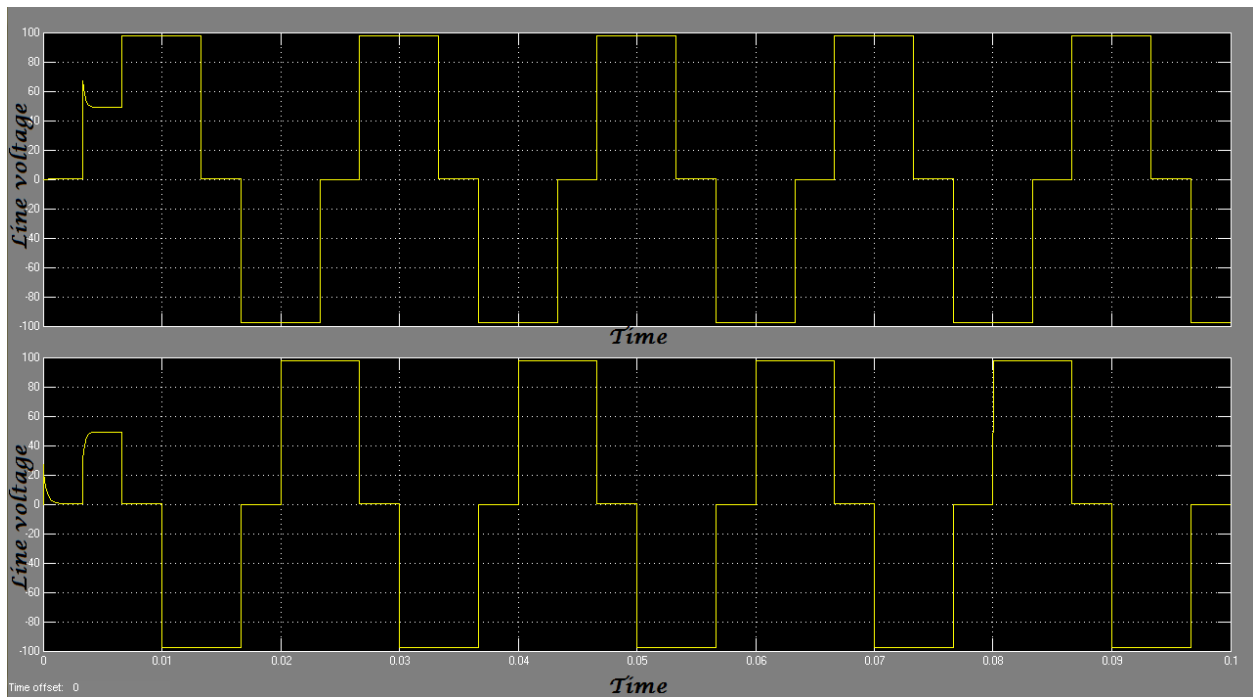


Fig. 4.2.2

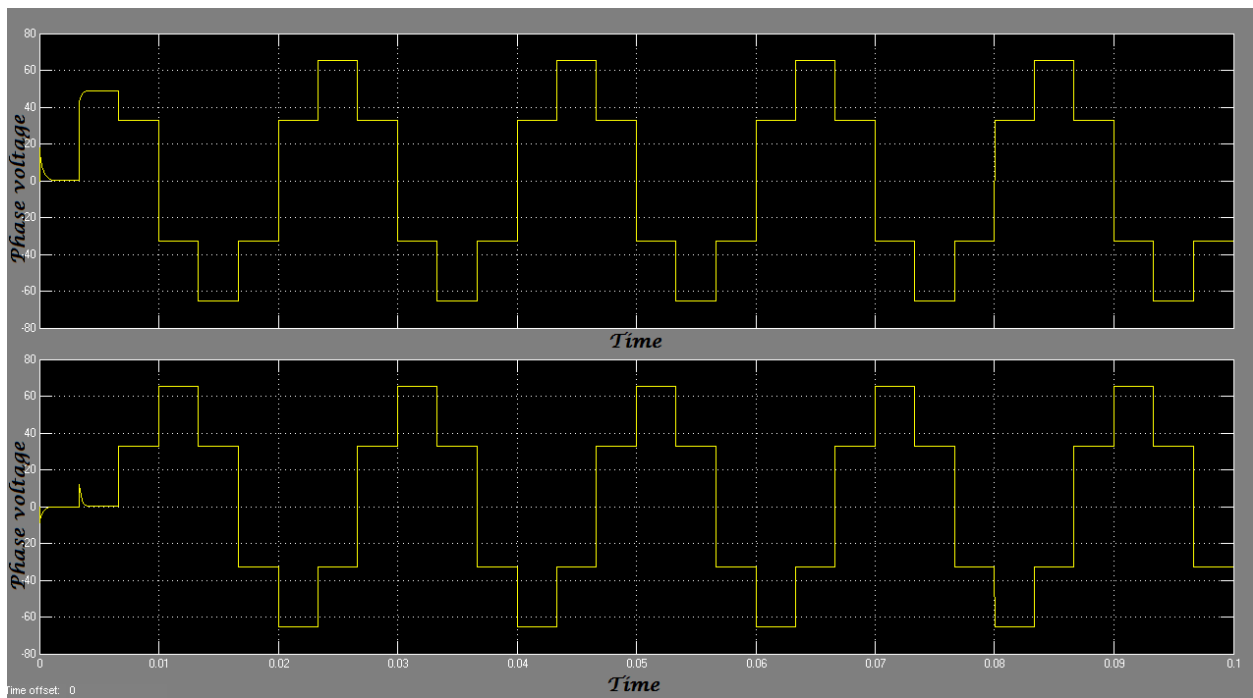


Fig. 4.2.3

4.3. MODELLING OF THE PV ARRAY

The PV cell model given in the SIMULINK library is a pre-existing source block in which the irradiation is constant at $1000\text{W}/\text{m}^2$. Thus it cannot be used for various levels of irradiation.

Hence an EMBEDDED MATLAB FUNCTION is used in which the code for solar block is used.

Below is the response it gives for various levels of insolation.

Each solar cell is rated to an open circuit voltage of 0.65V and short circuit current of 3.75A. The induction motor that is being used is of rating (440V, 7.5KW). Hence the number of cells required to be connected in series is 830 and number of such cells to be connected in parallel is 2. The solar cell is connected to an IRRADIANCE block that accounts for the solar radiation.

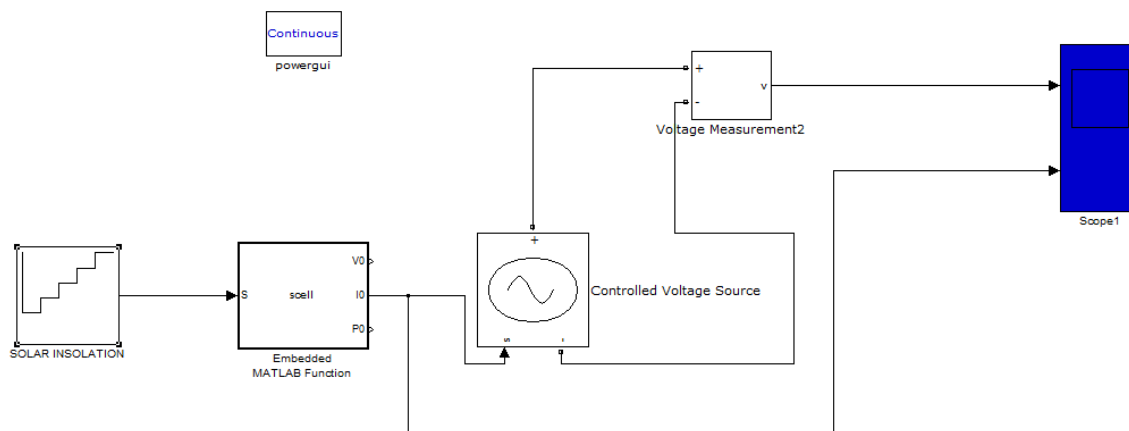


Fig. 4.3.1

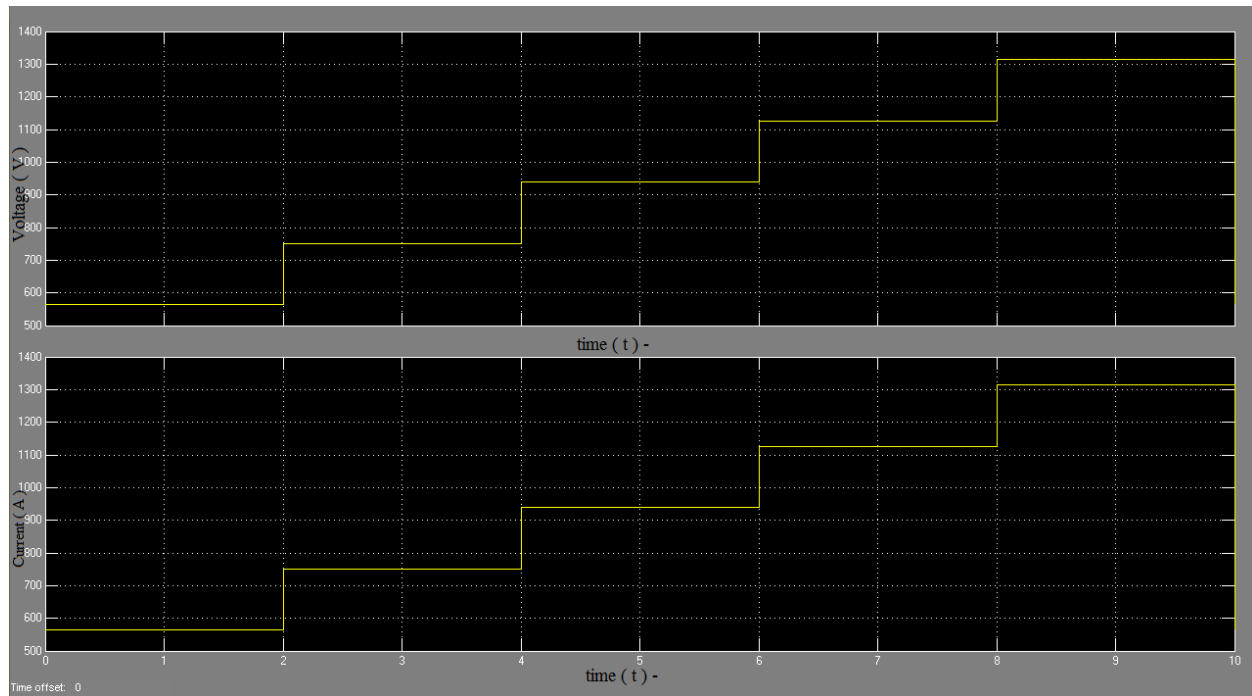


Fig. 4.3.2

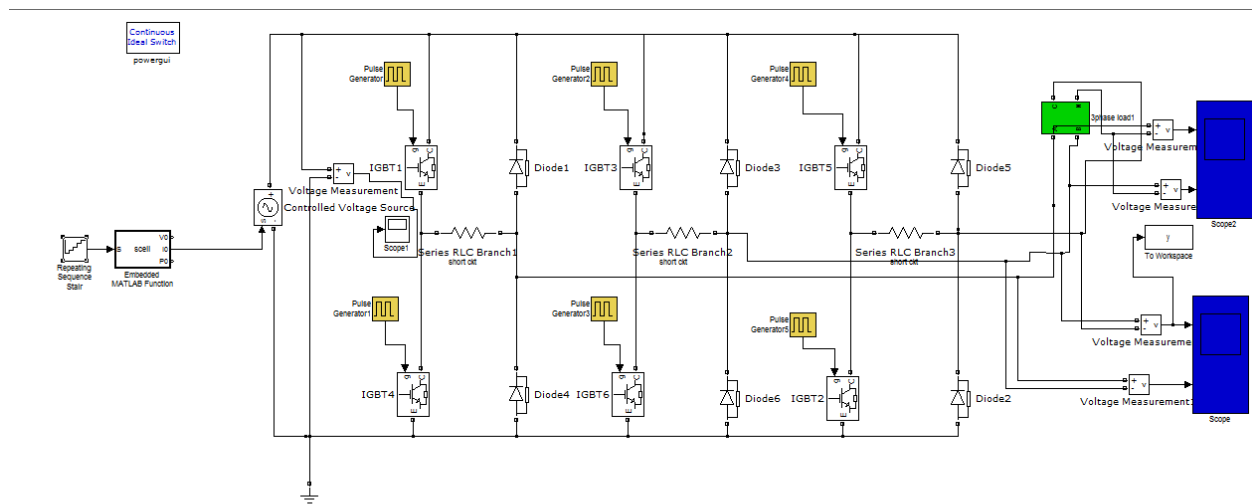


Fig. 4.3.3

When the PV array block connected to the inverter block is simulated it gives the similar output response as when the DC source of same magnitude is connected to the inverter block. This ensures that the model designed so far is right.

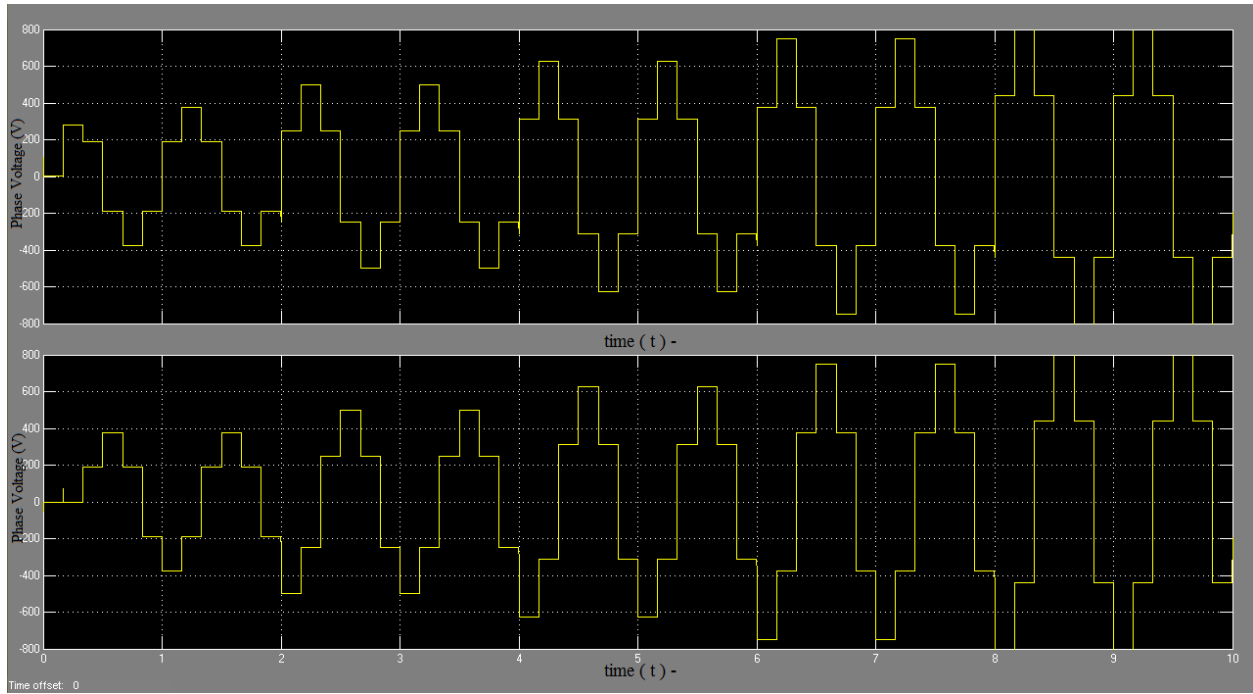


Fig. 4.3.4

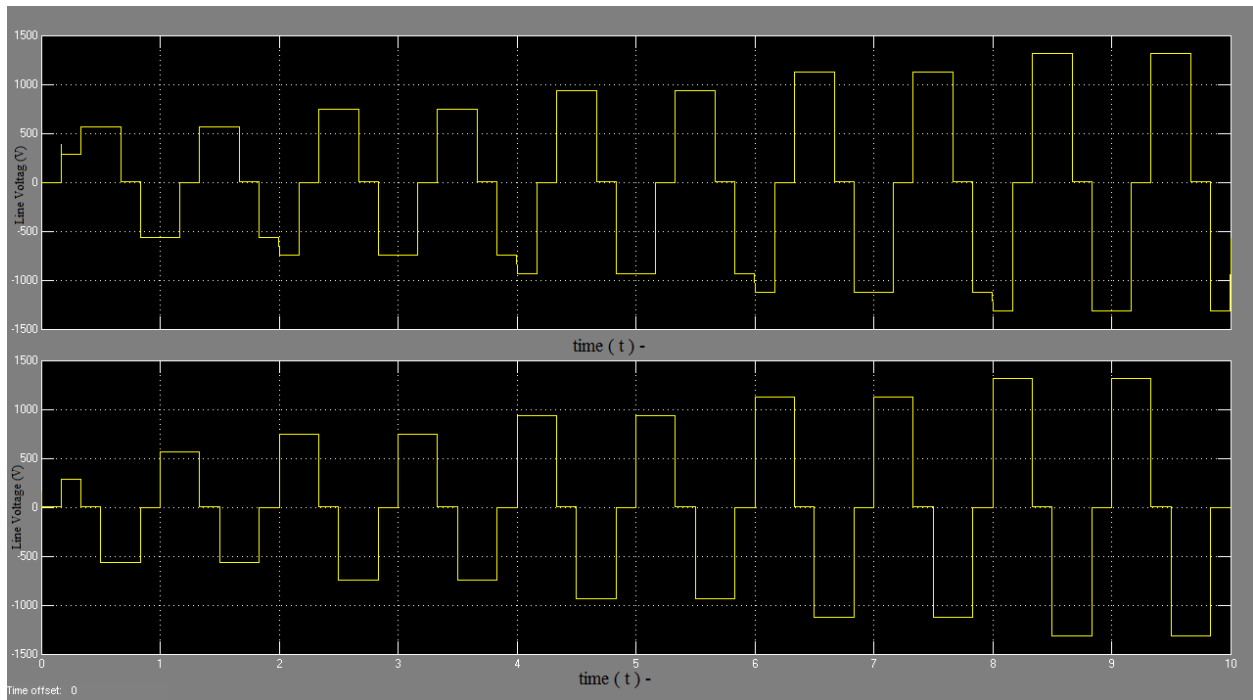


Fig. 4.3.5

4.4. CONNECTION OF MOTOR

When the motor is connected to the above model it is observed that the response is not appreciable. This is because the output obtained in the above model is a 6 step wave and contains a lot of harmonics which will definitely result in poor response.

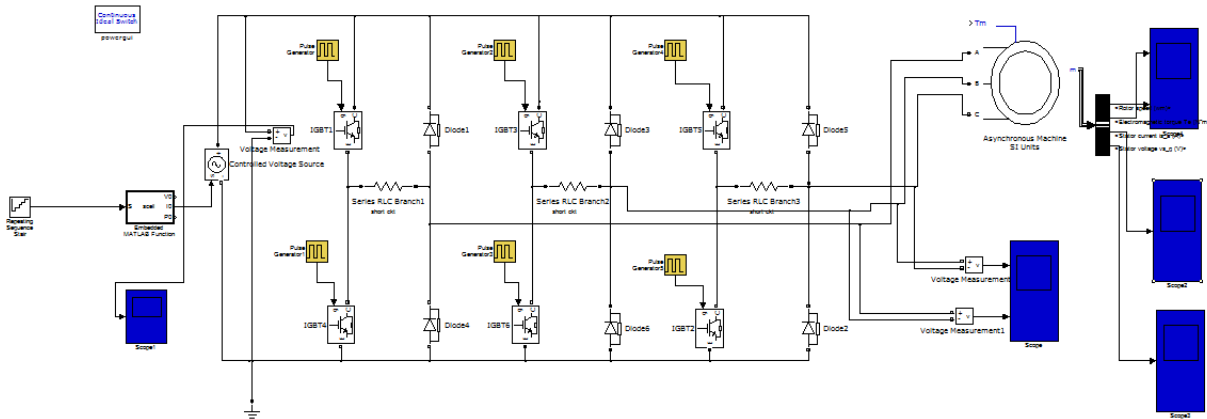


Fig. 4.4.1

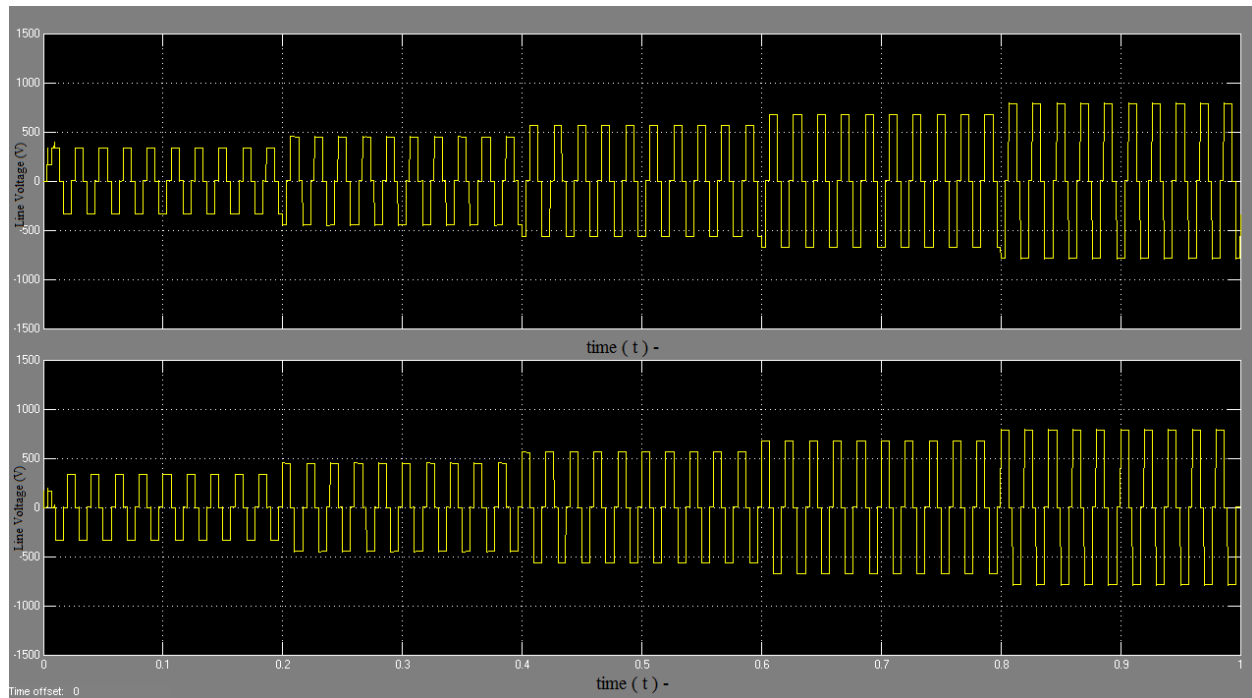


Fig. 4.4.2

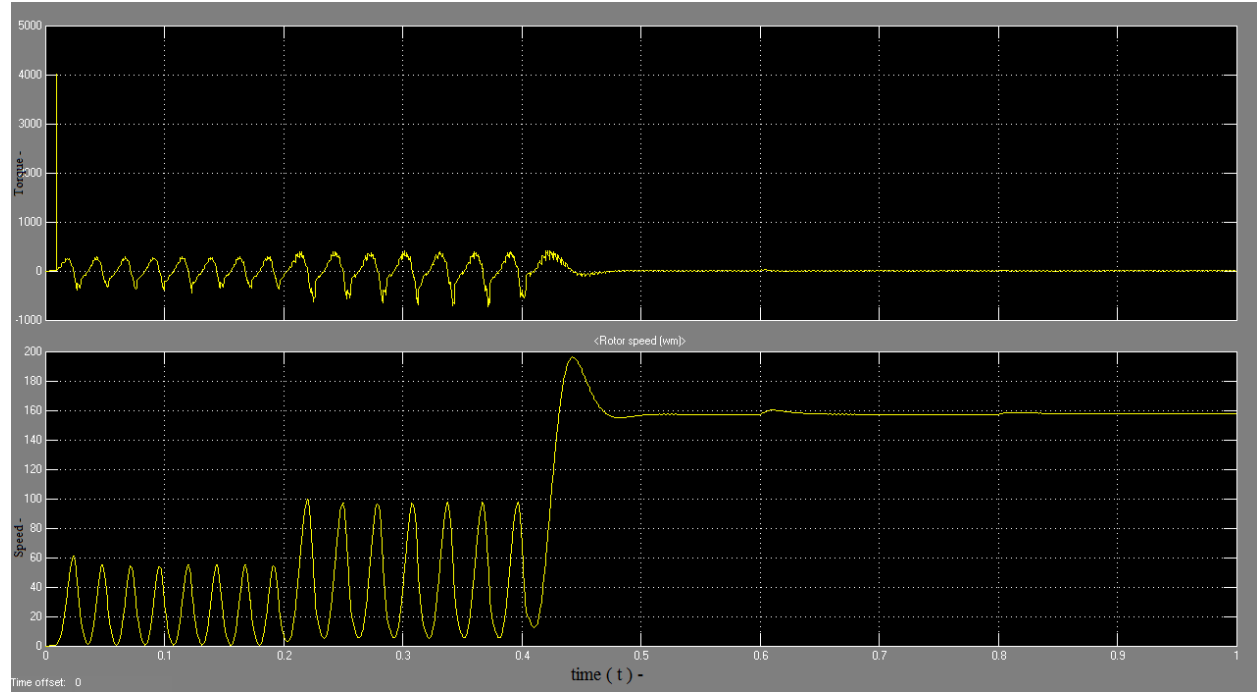


Fig. 4.4.3

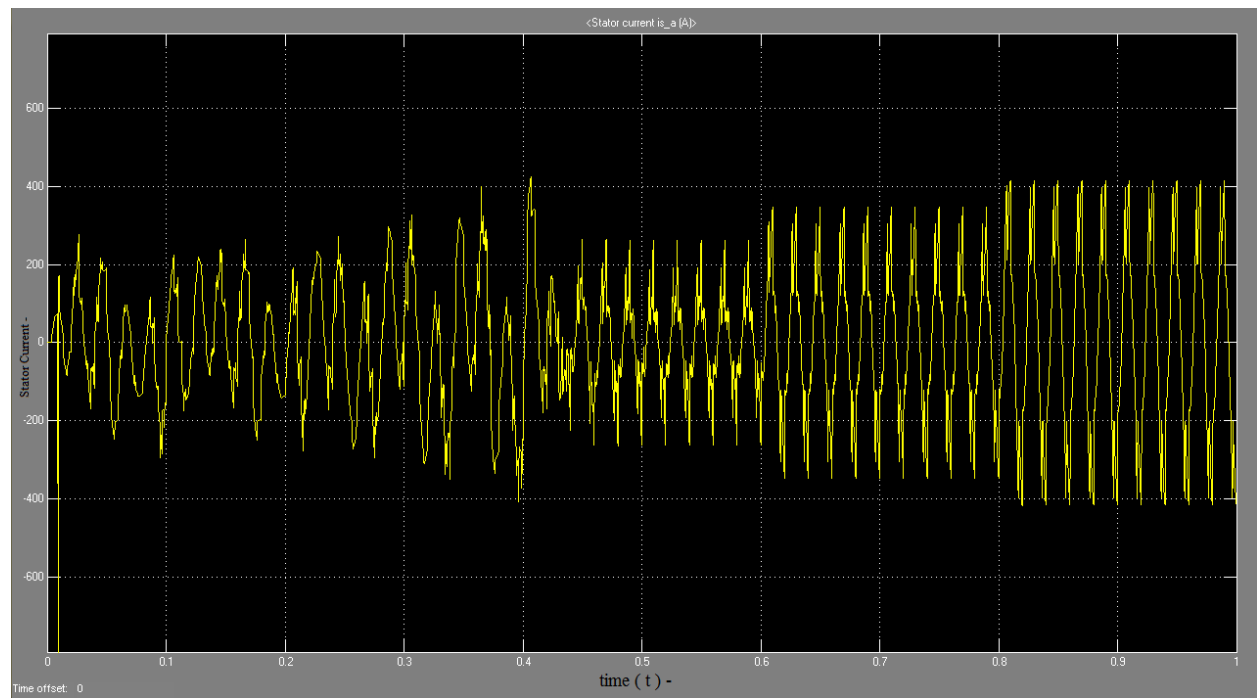


Fig. 4.4.4

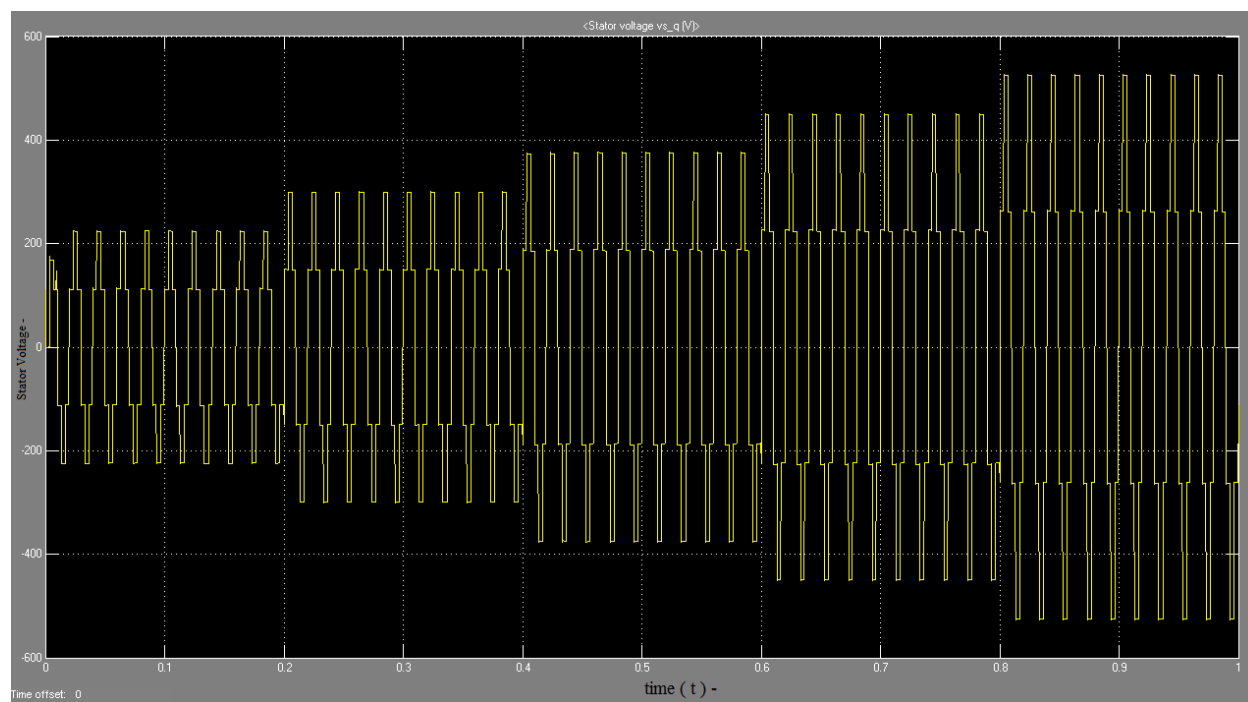


Fig. 4.4.5

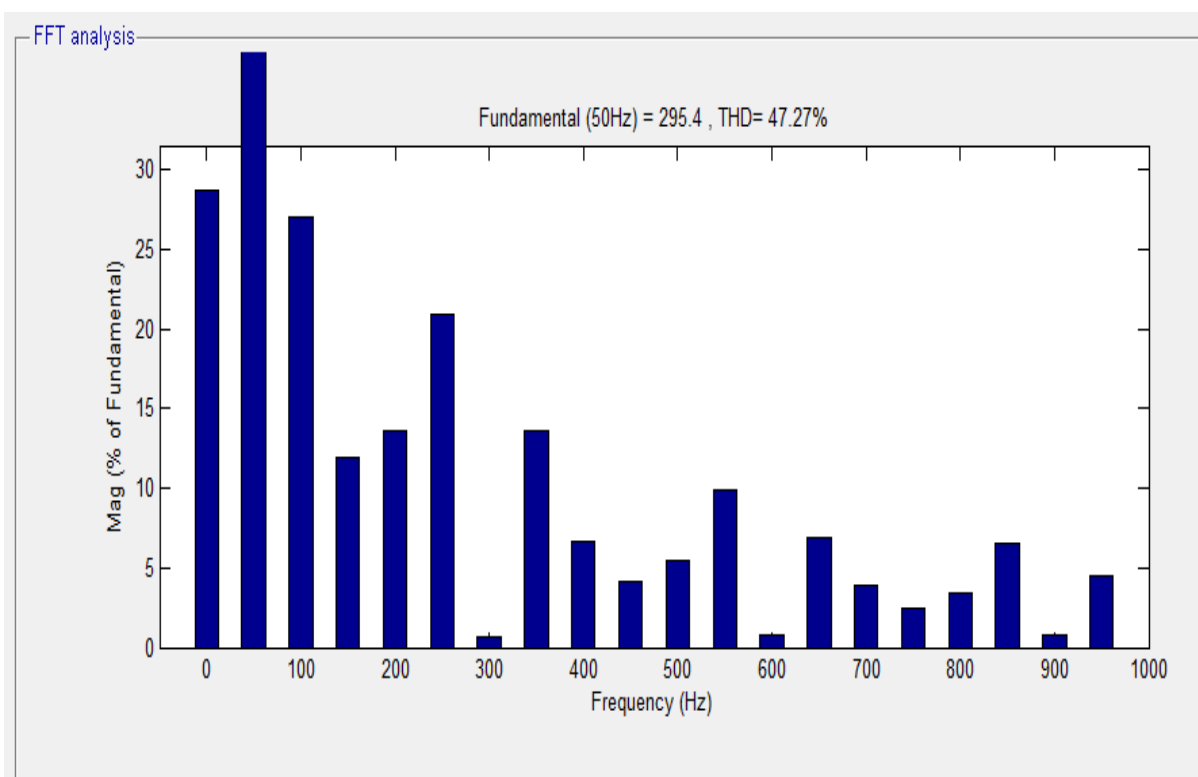


Fig. 4.4.6

4.5. DESIGN OF FILTER

To reduce the harmonic content in the output voltage of the inverter we require a filter. According to the FFT analysis the fundamental frequency that is required is 50 Hertz but other harmonics of higher order as well as the DC component are present. Thus we require a low pass filter whose cut-off frequency has been set to 52 Hertz. The response then obtained is a sine wave as required.

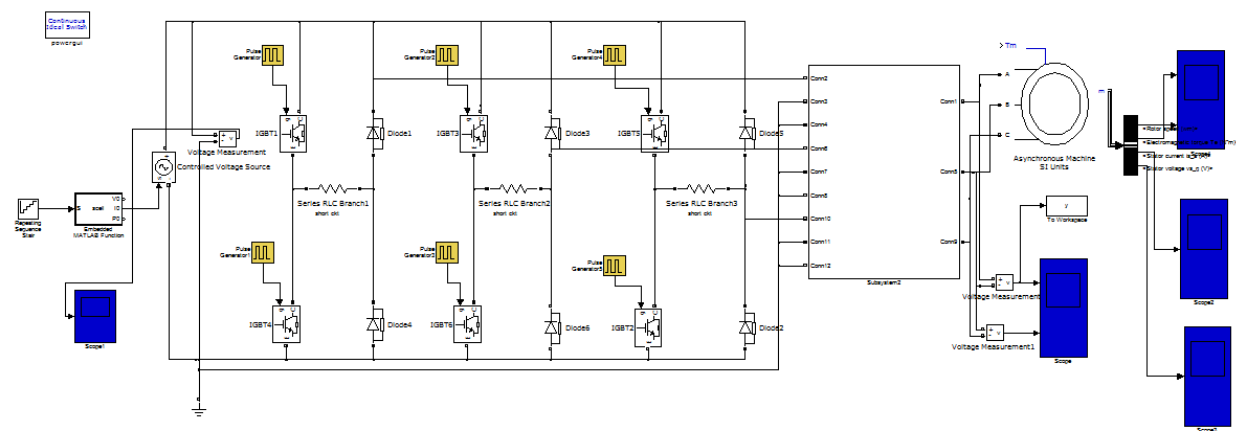


Fig. 4.5.1

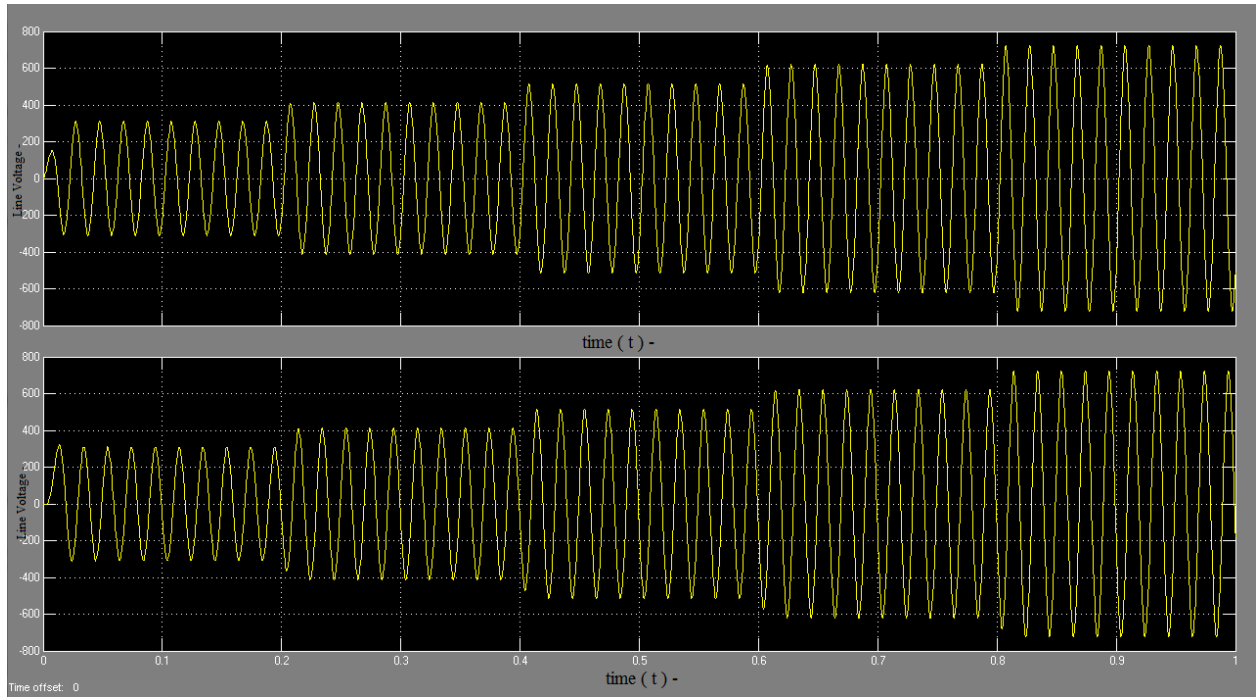


Fig. 4.5.2

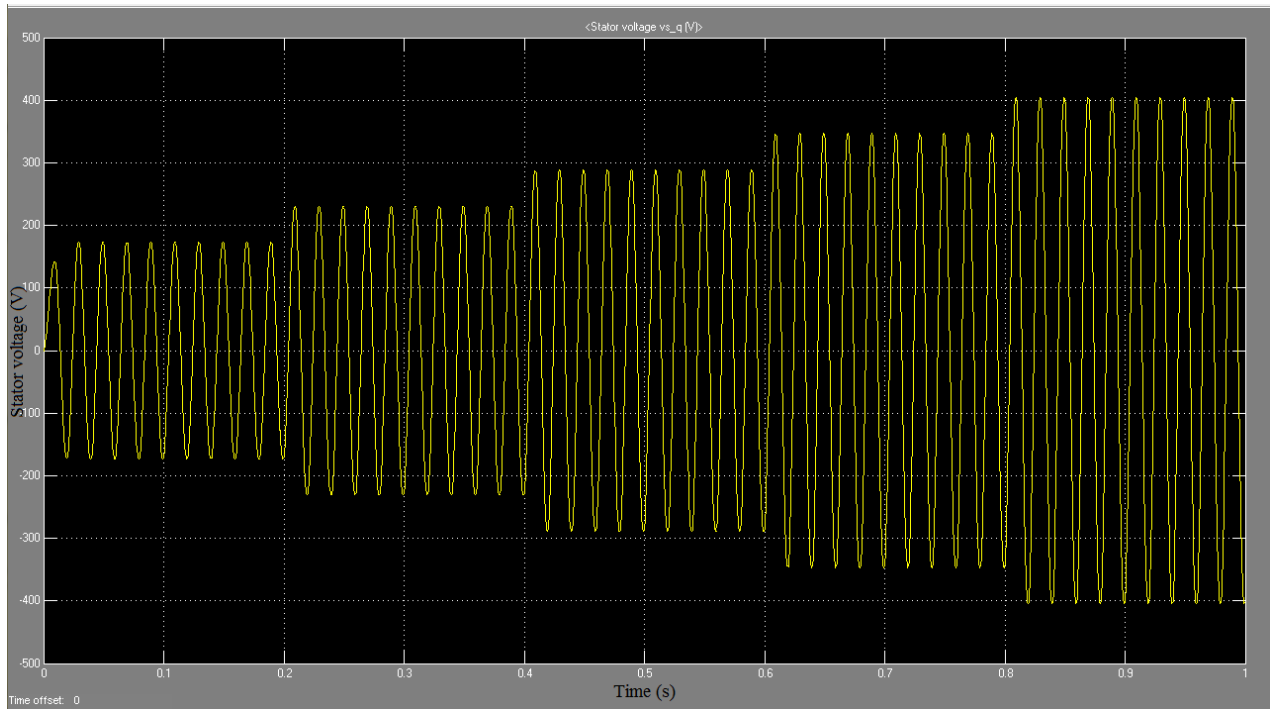


Fig. 4.5.3

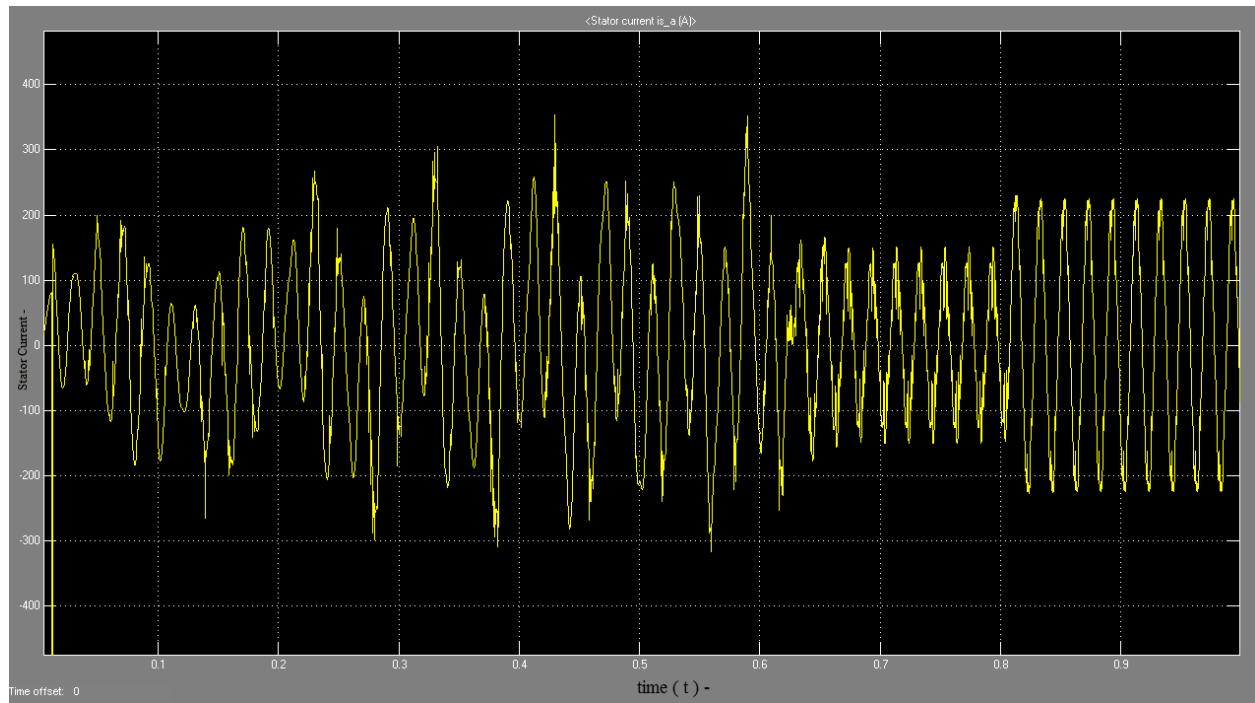


Fig.4.5.4

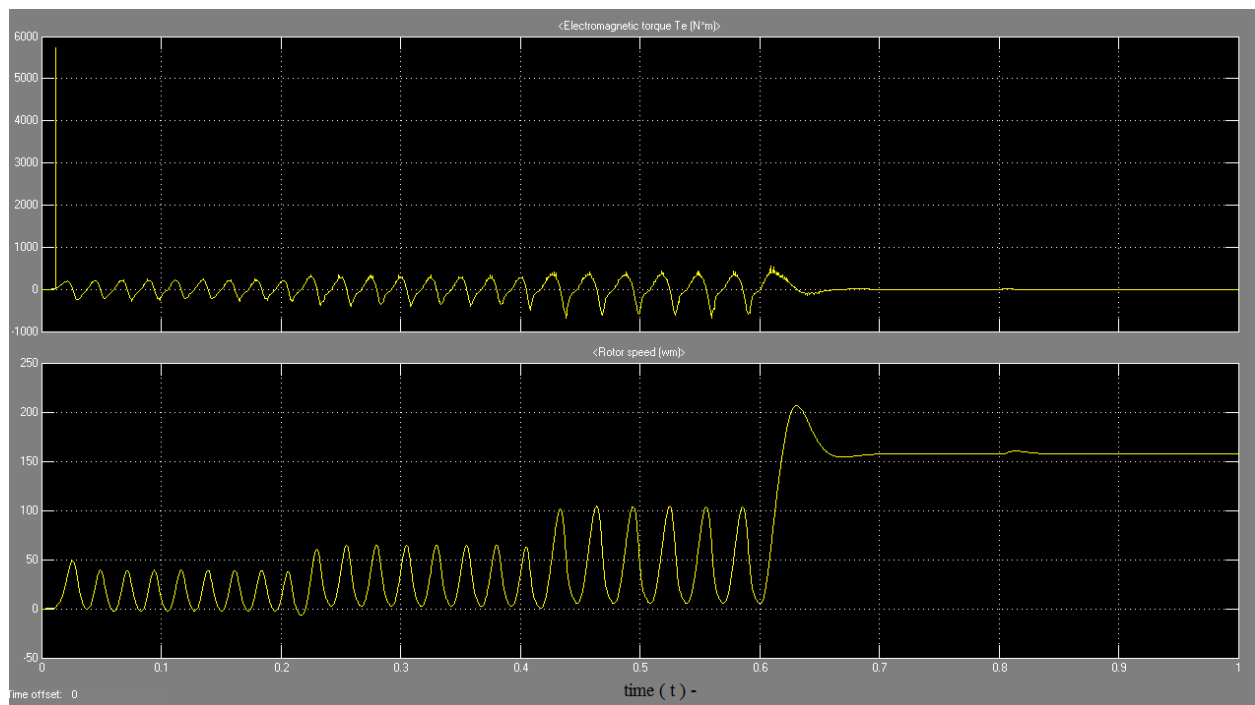


Fig. 4.5.5

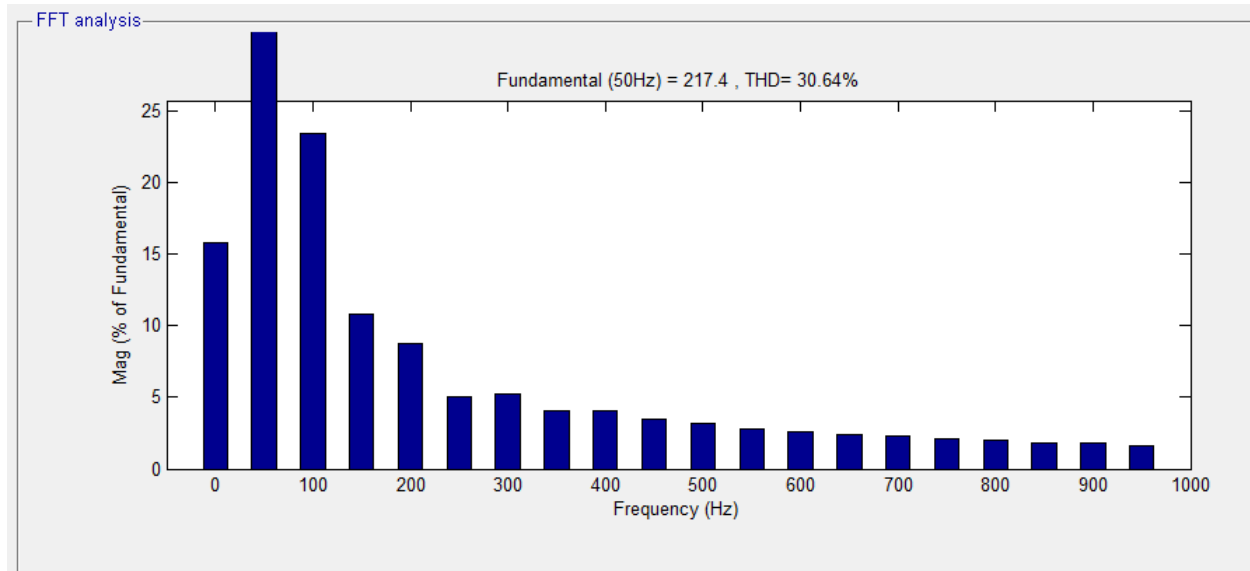


Fig. 4.5.6

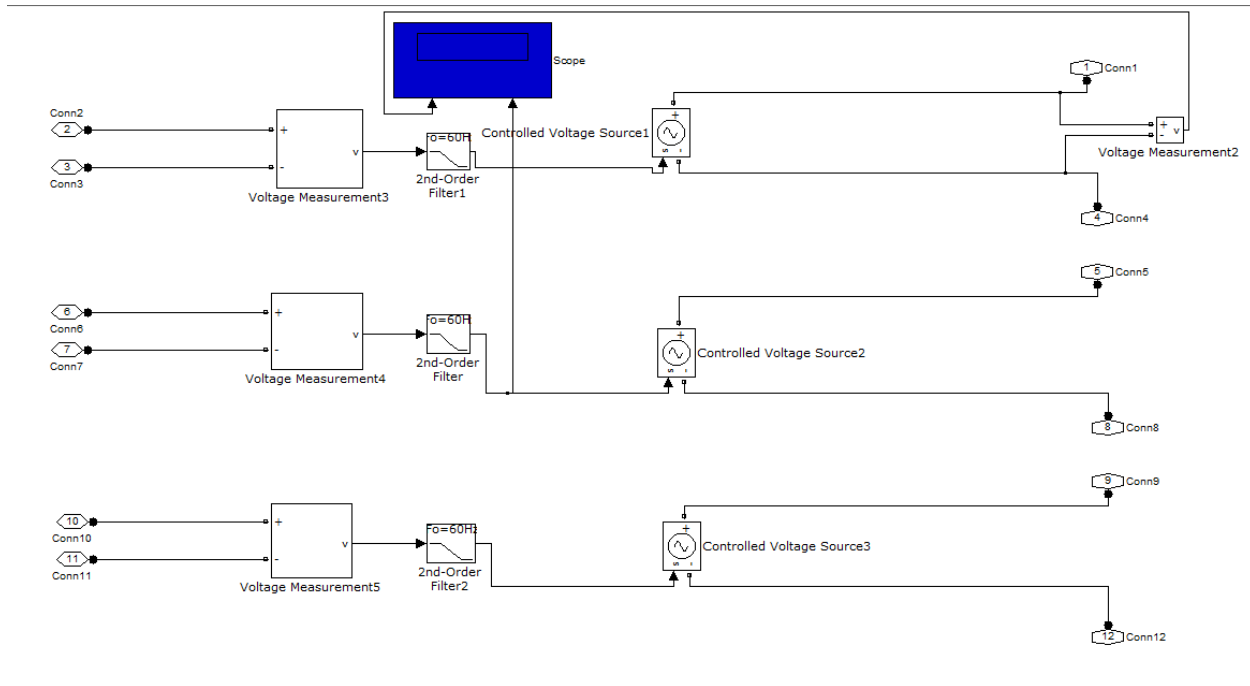


Fig. 4.5.7

4.6. CONNECTION OF CENTRIFUGAL PUMP

The torque output of the induction motor is connected to a torque actuator block that actuates the driveline axis and all connected inertias with torque specified by the incoming simulink signal in Nm. This torque actuator is connected on the other side to the rotational coupling that represents the rigid coupling between the driveline shaft and the simscape mechanical rotational shaft. It exchanges rotational kinetic energy between the driveline and the simscape without any loss. The rotational coupling is connected to the mechanical rotational conserving port associated with the pump driving shaft. The hydraulic conserving port inlet is connected to a reservoir while the outlet is connected to the variable head two arm tank that stores water under constant pressure. The scope measures the volume of water being pumped by the centrifugal pump out of the reservoir.

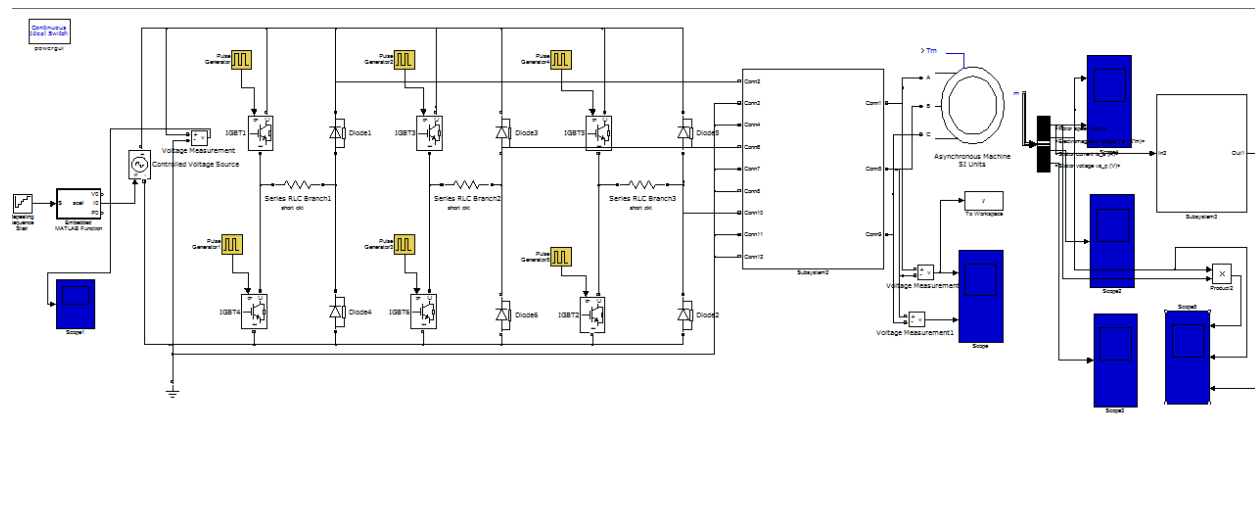


Fig. 4.6.1

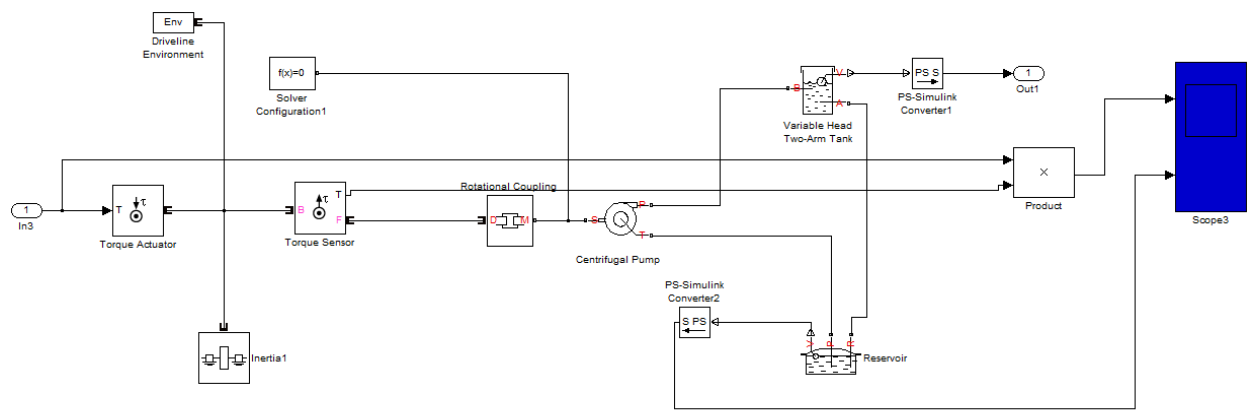


Fig. 4.6.2

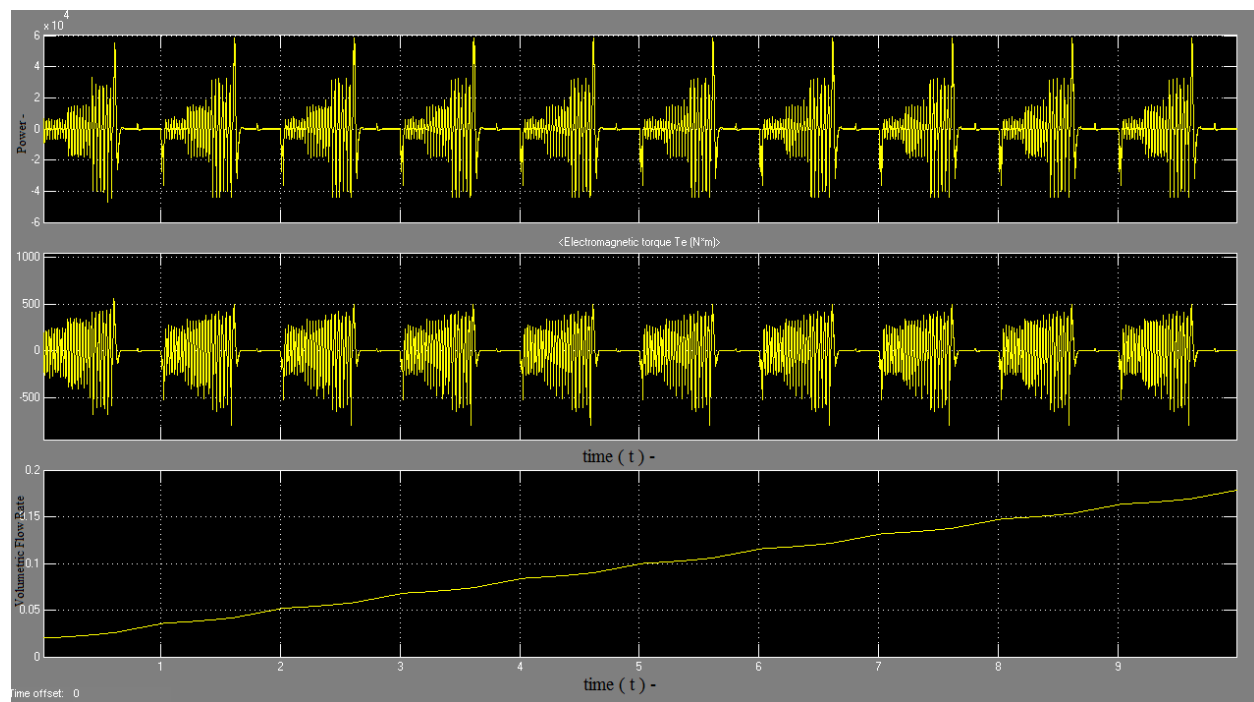


Fig. 4.6.3

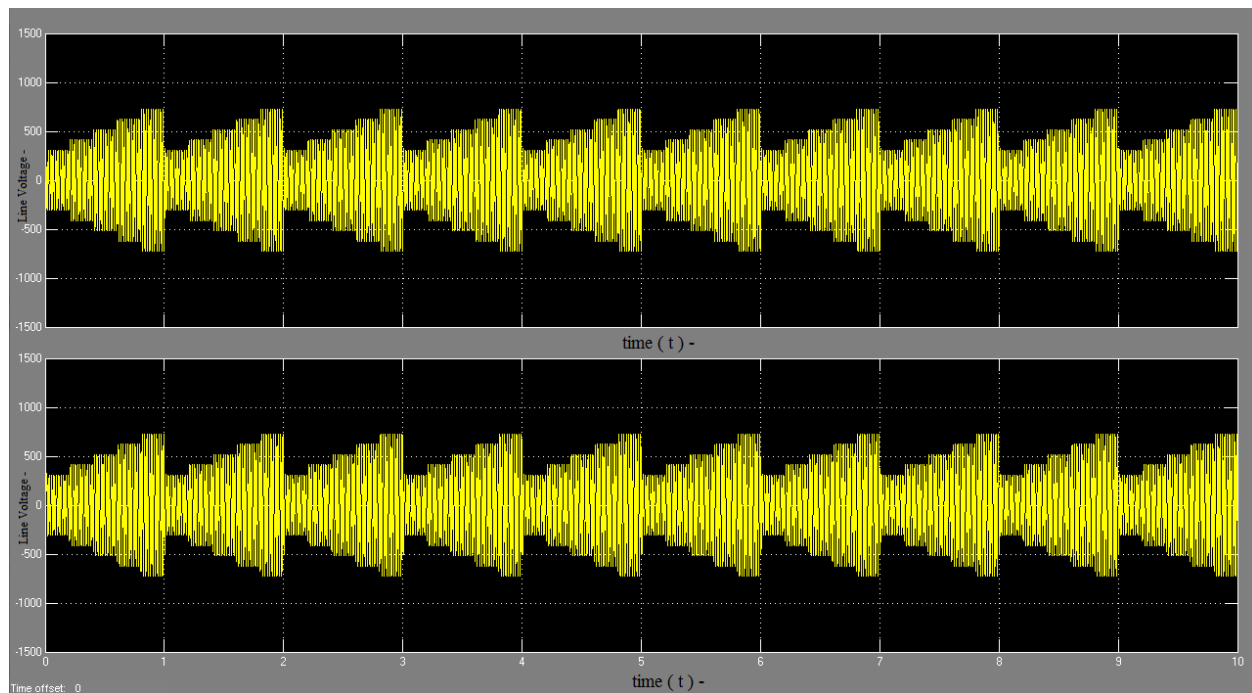


Fig. 4.6.4

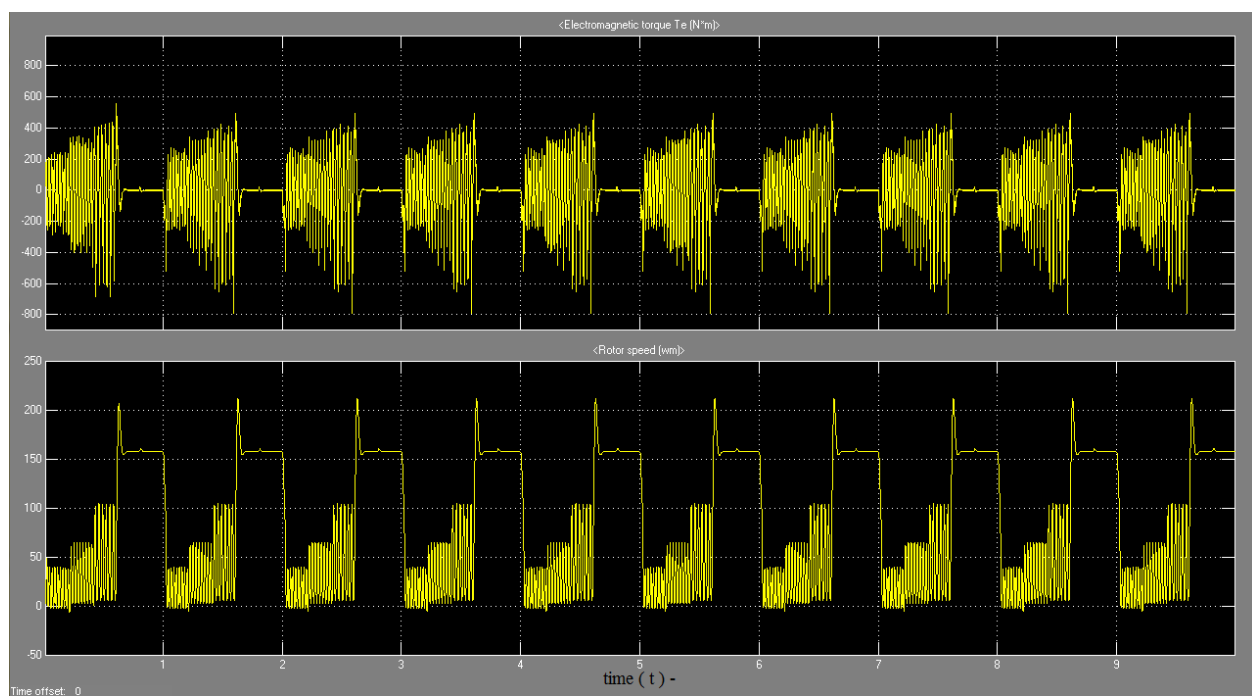


Fig. 4.6.5

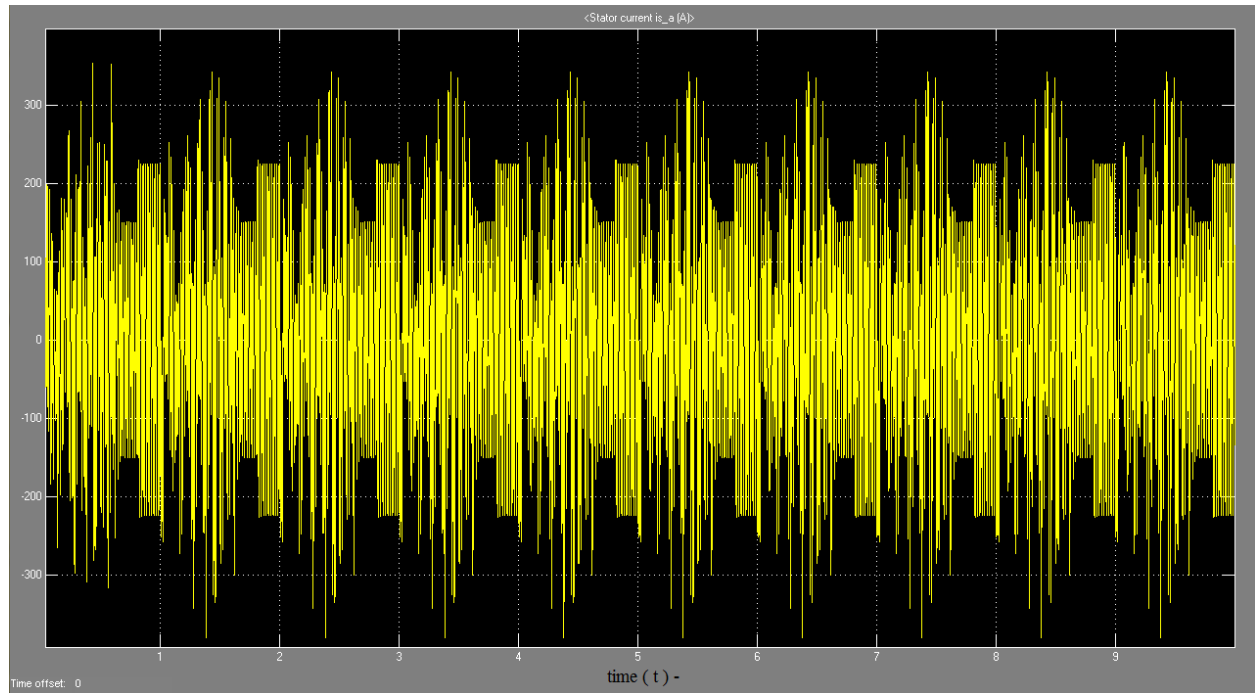


Fig. 4.6.6

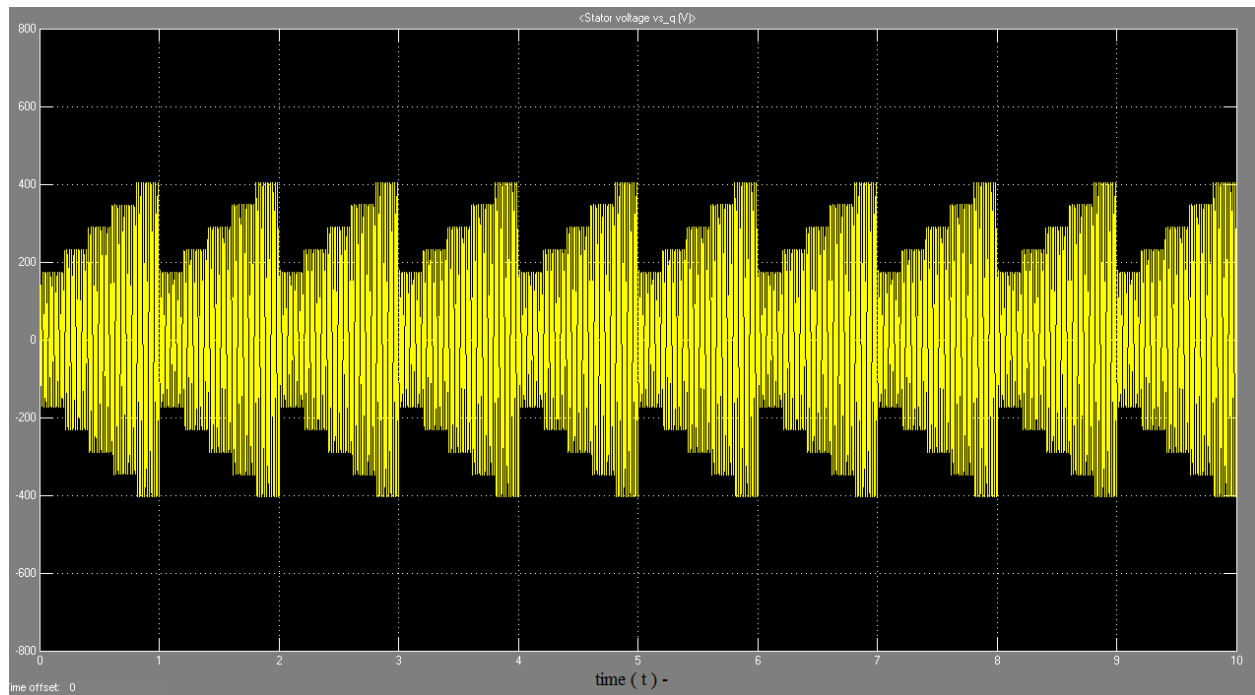


Fig. 4.6.7

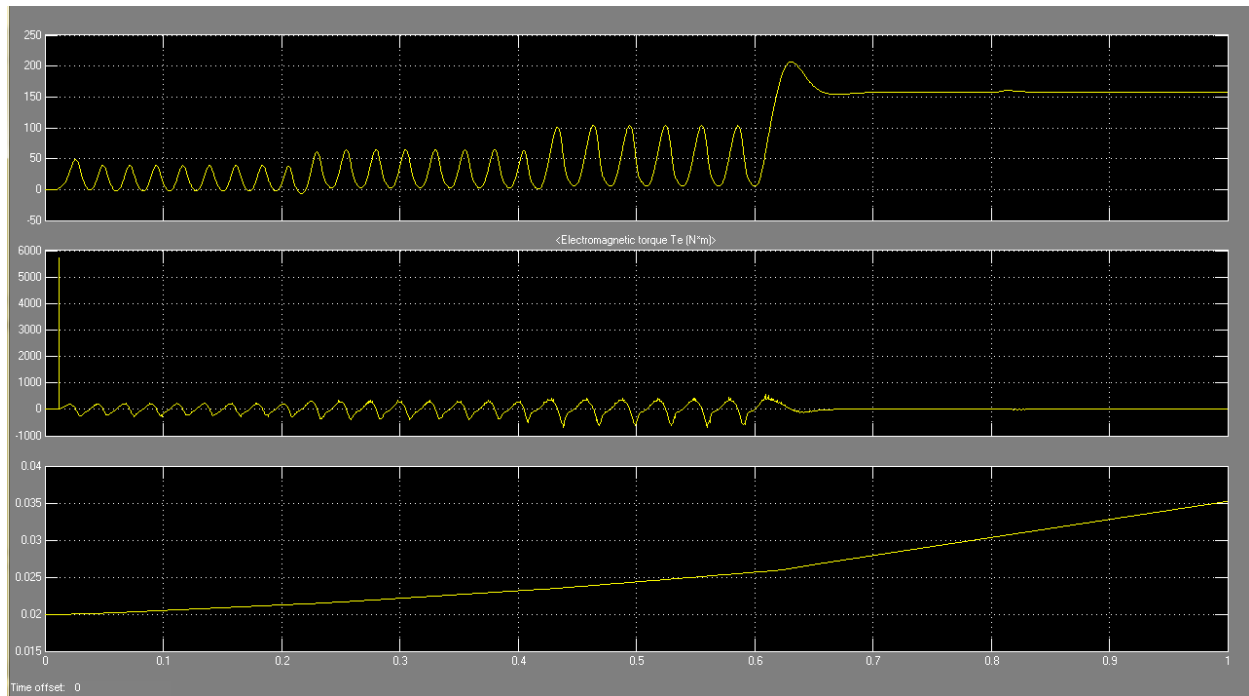


Fig.4.6.8

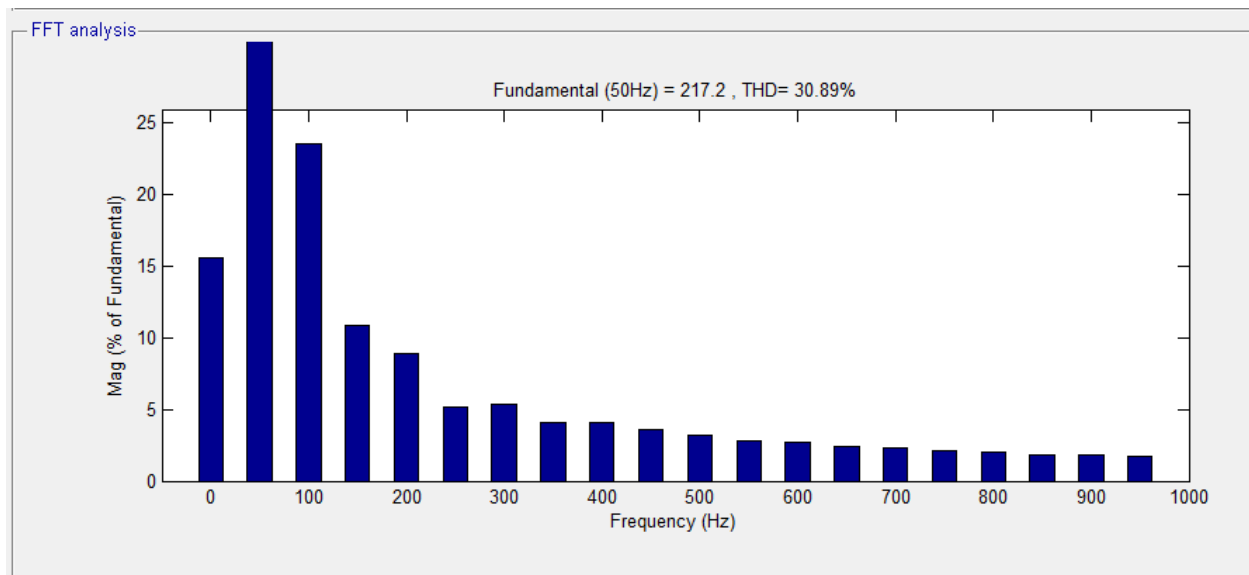


Fig. 4.6.9

4.7. IMPLEMENTATION OF THE CONTROL BLOCK

The control block is based on the algorithm mentioned in chapter 3. It helps increase the power input into the motor by varying the frequency of the inverter with respect to the change in insolation by calculating the short circuit current. The real implementation of the control block would require a microprocessor which would send the appropriate signal based on the insolation sensed by the sensor and fed into the microprocessor. In SIMULINK an EMBEDDED MATLAB FUNCTION has been used to serve the purpose. In addition to this a variable frequency programmable pulse generator has been used so that its time period and phase delay can be varied as per the demand.

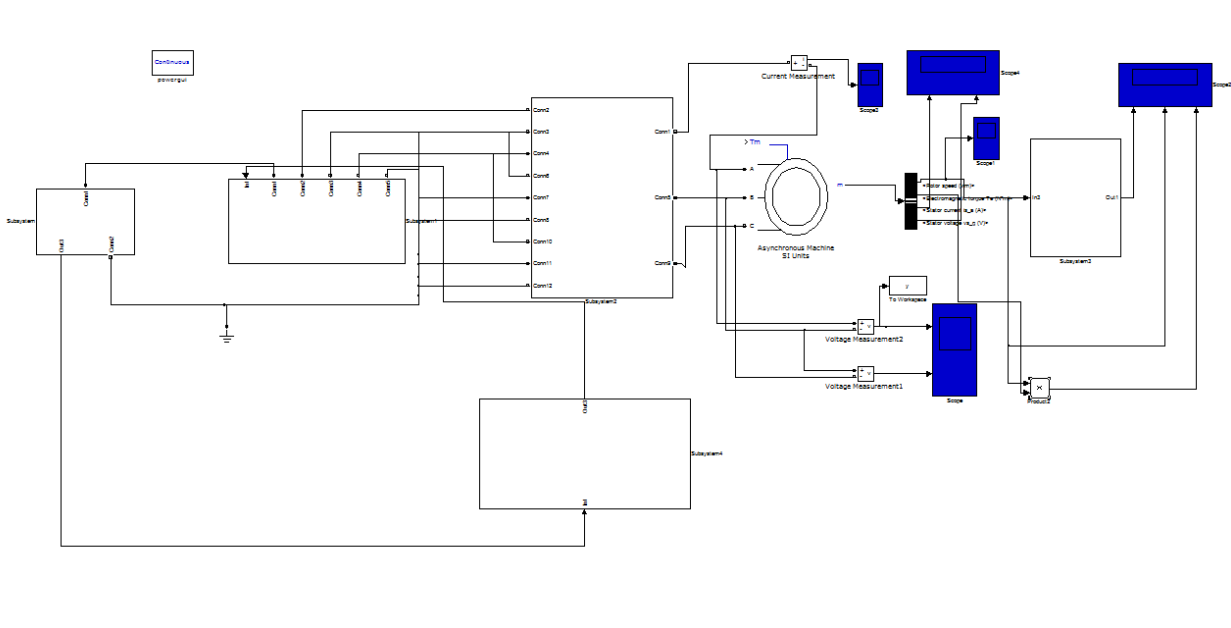


Fig. 4.7.1

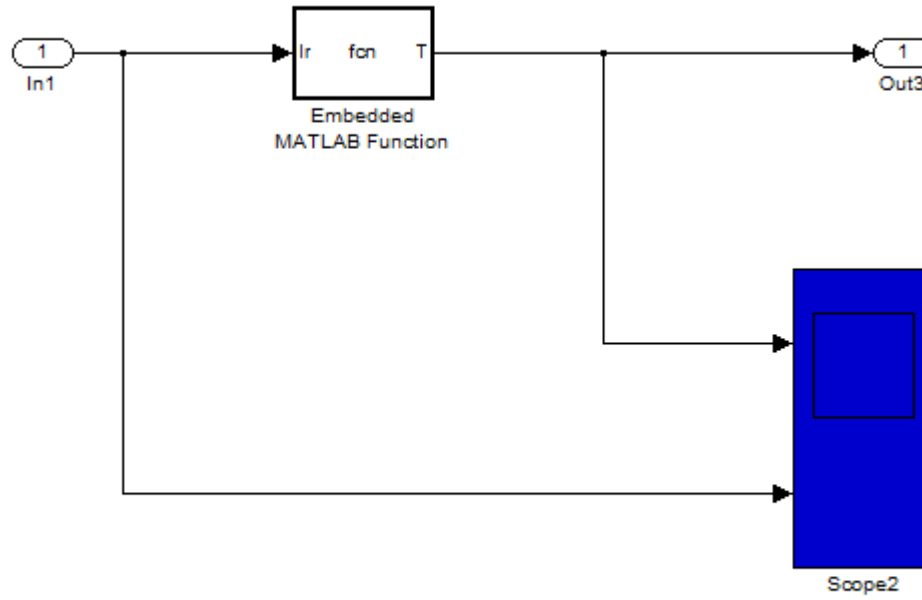


Fig. 4.7.2

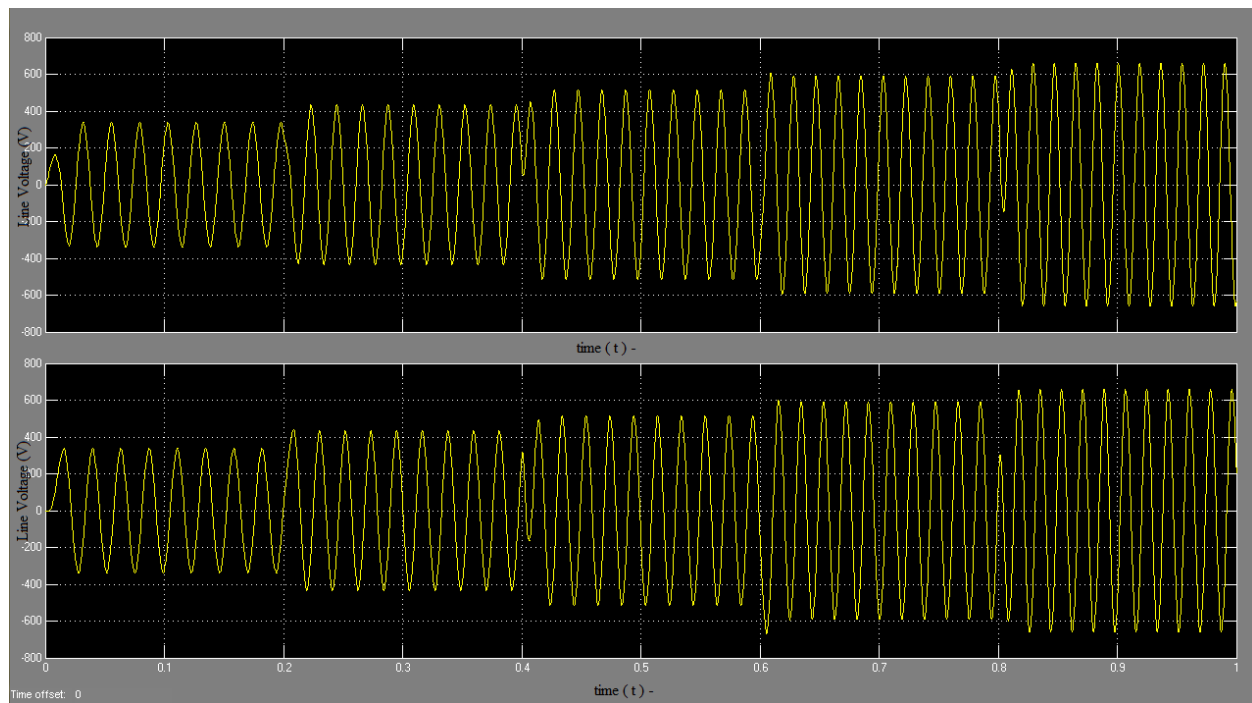


Fig. 4.7.3

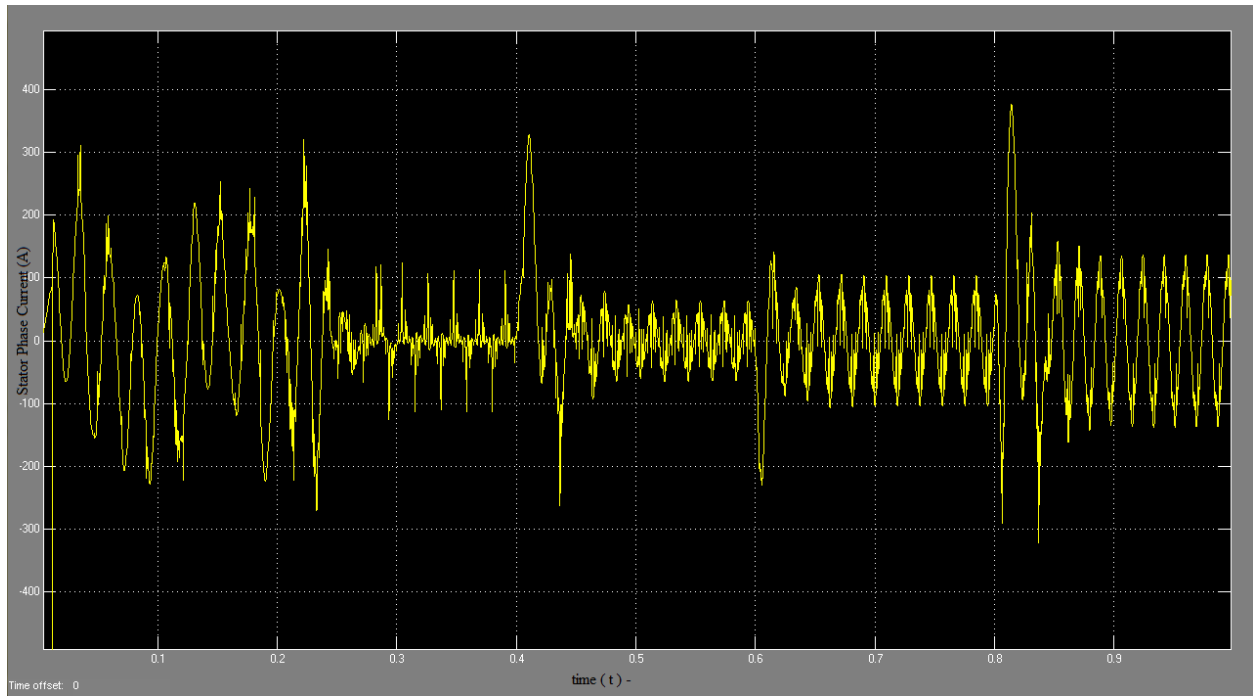


Fig. 4.7.4

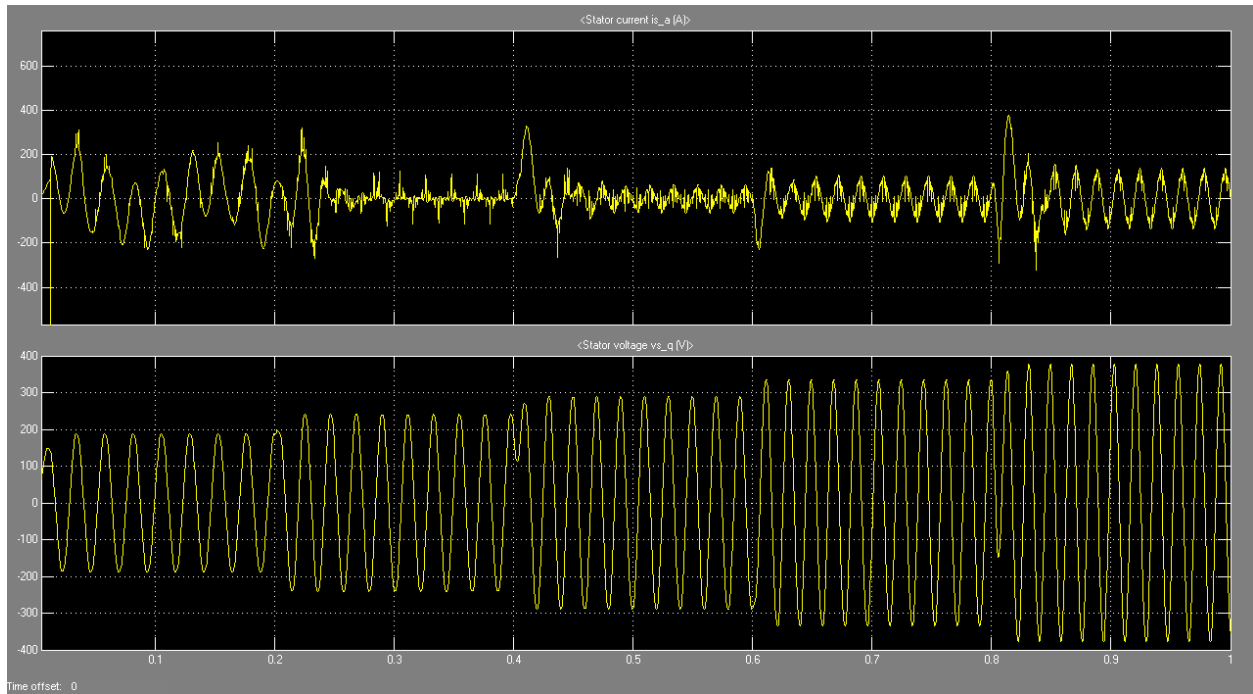


Fig. 4.7.5

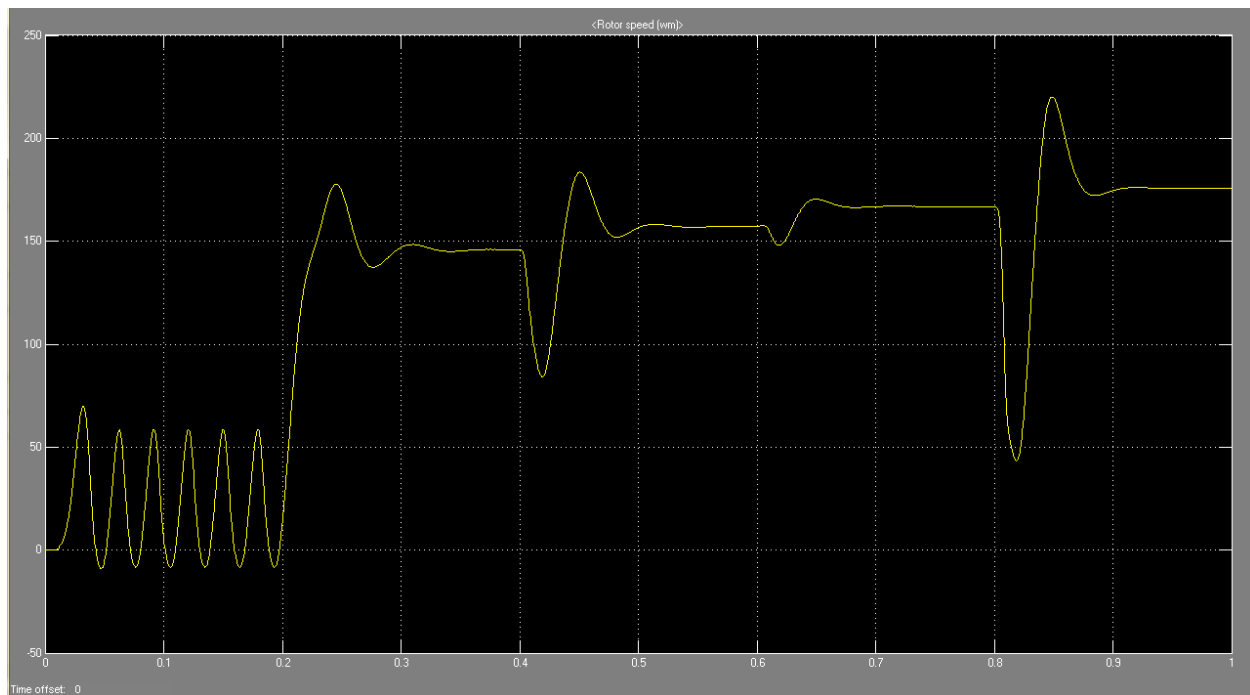


Fig. 4.7.6

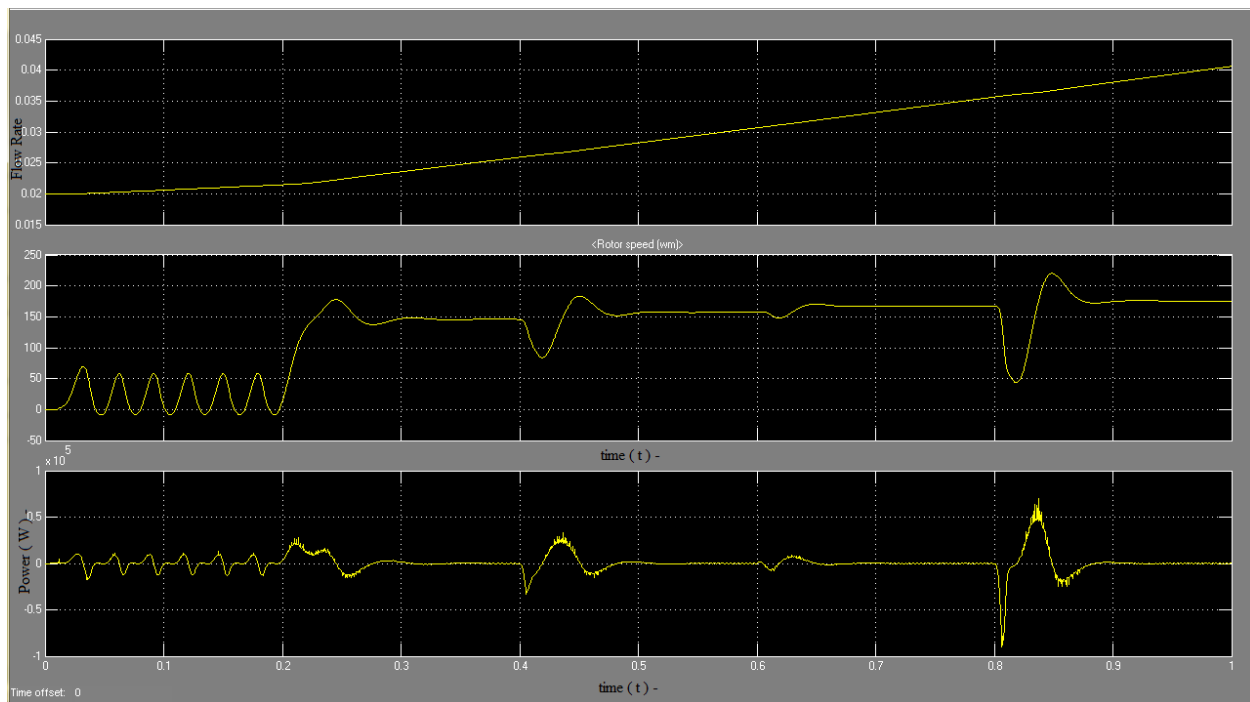


Fig. 4.7.7

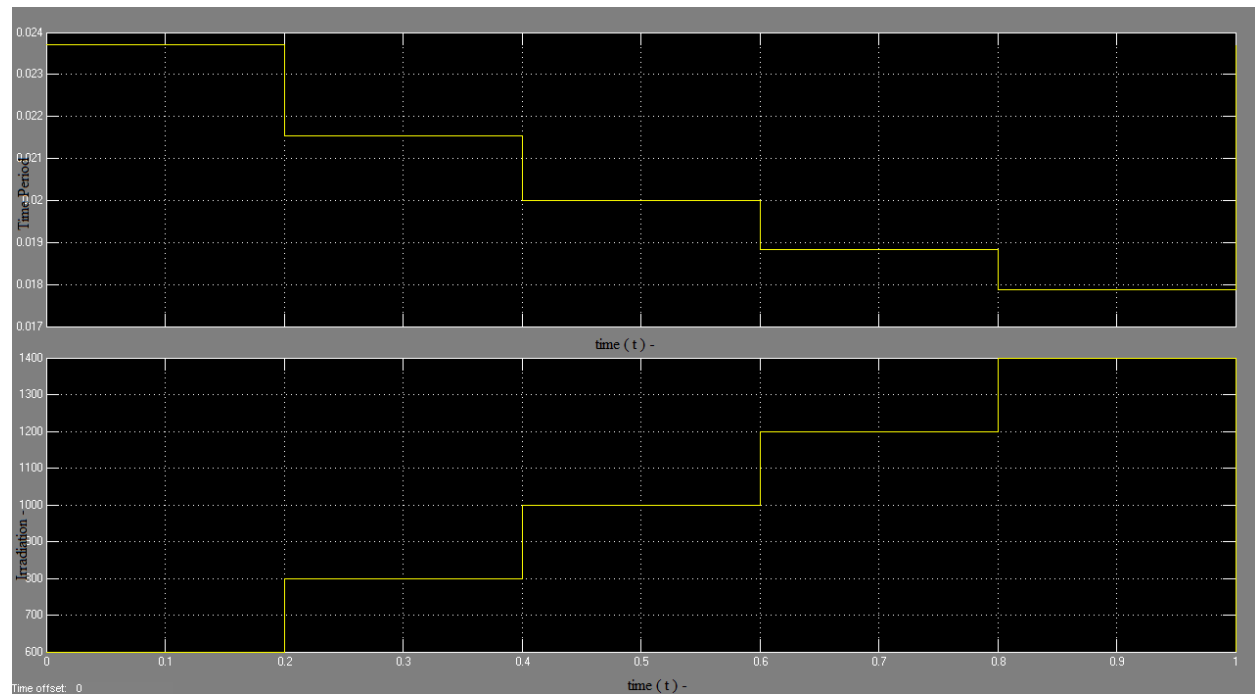


Fig. 4.7.8

CHAPTER 5

CONCLUSION

Under normal mode of operation the water pumping system when run under constant frequency the speed of the rotor, torque and the pump flow rate is as shown in Fig. 4.6.8. With the implementation of the control block the system's response increases. As per the theory the speed of the rotor must increase when the appropriate frequency is injected into the inverter. The results shown in Fig. 4.7.7 confirm the theory. With the increase in speed it can be implied that the pump power also increases. The increase in the pump volumetric flow rate shown in Fig. 4.7.7 confirms that the pump power is increased. Thus with the help of the given control algorithm the system's power and thus its efficiency at any given insolation can be increased.

REFERENCES:

- 1) Muljadi, Eduard. "PV Water Pumping with a Peak-Power Tracker Using a Simple Six-Step Square-Wave Inverter", IEEE TRANSACTIONS ON INDUSTRY APPLICATIONS, VOL. 33, NO. 3, MAY/JUNE 1997.
- 2) King, D.L.; Boyson, W.E.; and Kratochvil, J.A. (2004). "Photovoltaic Array Performance Model." 41 pp.; Sandia Report No. 2004-3535.
- 3) Nguyen, Dung Duc, "Modeling and reconfiguration of solar photovoltaic arrays under non-uniform shadow conditions" (2008). *Electrical Engineering Dissertations*. Paper 14.
- 4) Henderson, D.S. "VARIABLE SPEED ELECTRIC DRIVES - CHARACTERISTICS AND APPLICATIONS". IEE Colloquium on Energy Efficient and Environmentally Friendly Drive Systems - Principles, Problems and Applications (1996/144) .
- 5) Dr. Bimbhra, P.S. Power Electronics. New Delhi: Khanna Publishers, 2010.
- 6) Dr. Bansal, R.K. A Textbook of Fluid Mechanics and hydraulic machines. New Delhi: Laxmi publications Pvt. Ltd., 2010.
- 7) S. J. Butler, D. M. Sable, F. C. Lee, and B. H. Choo, "Design of a solar array simulator for the NASA EOS testbed," in *Proc. 27th Intersociety Energy Conversion Engineering Conf. (IECEC)*, San Diego, CA, 1992, pp. 1.63–1.66.
- 8) S. Cuk and R. D. Middlebrook, "Advances in switched-mode power conversion," in *Optimum Power Conversion*, vol. III. Pasadena, CA: Teslaco, 1993, pp. 325–345.
- 9) D. King, W. Boyson, and J. Kratochvil, "Analysis of Factors Influencing the Annual Energy Production of Photovoltaic Systems," 29th IEEE PV Specialists Conference, 2002.
- 10) C. Whitaker, T. Townsend, J. Newmiller, D. King, W. Boyson, J. Kratochvil, D. Collier, and D. Osborn, "Application and Validation of a New PV Performance Characterization Method," 26th IEEE PV Specialists Conference, 1997, pp. 1253-1256.